Implementation of Wireless Power Transmission System for Electric Vehicle Applications

A DISSERTATION

SUBMITTED IN PARTIAL FULFILLMENT OF THE REQUIREMENTS FOR THE AWARD OF THE DEGREE
OF

MASTER OF TECHNOLOGY
IN
POWER ELECTRONICS & SYSTEMS

Submitted by:
ABHISHEK SHAKYA
2K20/PES/02

Under the Supervision of

DR. MAYANK KUMAR

DEPARTMENT OF ELECTRICAL ENGINEERING
DELHI TECHNOLOGICAL UNIVERSITY
(Formerly Delhi College of Engineering)
Bawana Road, Delhi-110042

MAY, 2022

DELHI TECHNOLOGICAL UNIVERSITY
(Formerly Delhi College of Engineering)
Bawana Road, Delhi-110042

CANDIDATE'S DECLARATION

I, (Abhishek Shakya), 2K20/PES/02 student of M.Tech. (Power Electronics & Systems), hereby declare that the project Dissertation titled "Implementation of Wireless Power Transmission System for Electric Vehicle Applications" which is submitted by me to the Department of Electrical Engineering, Delhi Technological University, Delhi in partial fulfilment of the requirement for the award of the degree of Master of Technology, is original & not copied from any source without proper citation. This work has not previously formed the basis for the award of any Degree, Diploma Associateship, Fellowship or other similar title or recognition.

Place: Delhi   **Abhishek Shakya**

Date: **2K20/PES/02**

DEPARTMENT OF ELECTRICAL ENGINEERING
DELHI TECHNOLOGICAL UNIVERSITY
(Formerly Delhi College of Engineering)

Bawana Road, Delhi-110042

CERTIFICATE

I hereby certify that the Project Dissertation titled "Implementation of Wireless Power Transmission System for Electric Vehicle Applications" which is submitted by [Abhishek Shakya], 2K20/PES/02 [Department of Electrical Engineering], Delhi Technological University, Delhi in partial fulfilment of the requirement for the award of the degree of Master of Technology, is a record of the project work carried out by the students under my supervision. To the best of my knowledge this work has not been submitted in part or full for any degree or Diploma to this University or elsewhere.

Place: Delhi

Assistant Professor Dr. Mayank Kumar

Date:

SUPERVISOR

DEPARTMENT OF ELECTRICAL ENGINEERING

DELHI TECHNOLOGICAL UNIVERSITY
(Formerly Delhi College of Engineering)

Bawana Road, Delhi-110042

ACKNOWLEDGMENT

I wish to express our sincerest gratitude to **Dr. Mayank Kumar** for his continuous guidance & mentorship that he provided me during the project. He showed us the path to achieve my target by explaining all the tasks to be done & explained to me the importance of this project as well as its industrial relevance. He was always ready to help me and clear my doubt regarding any hurdles in this project. Without his constant support and motivation, this project would not have been successful.

I would like to thank my friends, seniors and all those who have directly or indirectly helped me in completion of the thesis well in time. Finally, I wish to thank my parents for their moral support and confidence showed in me to pursue M.Tech at an advanced stage of my academic career.

Place: Delhi   Abhishek Shakya

Date:

ABSTRACT

The goal of this study is to see if an inductive-coupled Wireless Power Transfer (WPT) System can be used for electric vehicle charging in MVDC power networks. WPT in electric vehicles (EVs) can provide a more convenient charging option than static charging in a station, which can take hours. It can also reduce the risk of electrocution from the use of physical media such as wires in EV charging. Despite the fact that inductive coupling has been used in some WPT applications, it is still inefficient for transferring high power at the kilowatt level due to weak coupling between the transmitter and receiver. Using correctly configured resonant circuits in conjunction with inductive coupling can improve coupling and make the system more efficient.

The goal of this study is to construct and evaluate a 2-KW WPT circuit. A resonant circuit's optimal specification is investigated and described. The component values in the circuit are determined using theoretical calculations. The WPT system is validated in a MATLAB/SIMULINK environment.

NOMENCLATURE

AC	Alternating Current
DC	Direct Current
WPT	Wireless Power Transfer
EV	Electric Vehicle
MVDC	Medium Voltage Direct Current
ICE	Internal Combustion Engine
IPT	Inductive Power Transfer
CPT	Capacitive Power Transfer
HEV	Hybrid Electric Vehicle
PHEV	Plug in Hybrid Electric Vehicle
PWM	Pulse Width Modulation
MOSFET	Metal oxide semiconductor field effect Transistor

TABLE OF CONTENTS

LIST OF TABLES

LIST OF FIGURES

CHAPTER 1

INTRODUCTION

1.1 INTRODUCTION

Electric Vehicles (EVs) have become more popular in recent decades as a result of their benefits over ICE vehicles. The EVs emits far low carbon-dioxide, which helps to mitigate global warming to a large extent. EVs have wound up various stages of evolution in terms of topology related to its design and in-built technology since their origination. The purpose of this work is to build and analyse the wireless power transfer (WPT) topology based on inductive coupling for electric vehicles (EVs) to connect along the MVDC networks. The main focus of the design will be on the study and analysis of a resonant circuit topology for use in a wireless inductive power transfer (IPT) system.

The number of personal automobiles is predicted to rise at the current rate of technological and urbanisation development. Because the majority of vehicles on the road now run-on fossil fuels, one can see the problems that oil use might cause society. It has the potential to cause global warming, bad air quality, and a few political confrontations. Every day, the world consumes about 85 million barrels of oil. Transportation accounts for 60% of total oil use, with the United States accounting for 25% of that. It has been established that only 1300 billion barrels are accessible for additional use, implying that oil will be scarce in 40 years. EVs have the potential to play a significant role in averting this [1].

Even if electric vehicles are outperforming common ICE vehicles in terms of energy efficiency and persistent viability, the use of a physical medium for power transmission may be harmful at times. In truth, electric vehicles were conceived in 1895, but a number of circumstances influenced the EV market, leading to their demise in 1930. The following are a few of the most important factors.

1) EVs took about 8 hours or more to charge, which is quite long. EVs were 40 percent more expensive than ICE automobiles.

2) In comparison to ICE vehicles, operating and maintenance costs for electric vehicles were considerable.

3) Despite the lack of evidence that EVs are risky than ICE vehicles, manufacturers of automobile were hesitant to invest in EV research, development, and manufacturing due to a market downturn at the time.

4) In the 1990s, most EVs had lead acid batteries, which were very heavy and required a long charging period. There was also a lack of adequate infrastructure for charging electric vehicles.

5) Hybrid electric vehicles (HEVs) and the Plug-in Hybrid Electric Automobiles (PHEVs) were also more expensive than gasoline-powered vehicles.

Even in recent years, electric vehicles have been limited by energy storage technologies. Batteries have a low energy density, a short lifespan, and are therefore more expensive. Expanding a typical conveyance electric bus is tough due to the cost and battery size. In a bus, the battery may account for up to 39% of the entire cost, and it can weigh up to 26% of the total weight. It's difficult to create a battery with appropriate energy and power density, safety and dependability. Furthermore, charging the automobile for the first time can take anything from half an hour to several hours depending on the charger's power level [2]. Fast-charging batteries have been proposed as a solution to this problem; however, these batteries have a high charge acceptance and are not suited for use in cars. Furthermore, in stormy weather, it may increase the risk of electric shock. EV users are growing more interested in WPT vehicles as a result of these disadvantages. By lowering the size of your battery, wireless charging may help you save time and space [3,4].

Electric vehicles can be employed as energy storage units in vehicle-to-grid (V2G) and traditional grid-to-vehicle (G2V) charging applications, in addition to addressing environmental degradation and the fossil fuel problem [5, 6]. The primary concept behind V2G technology is to employ automobiles as energy storage devices that give electricity to the grid during voltage and frequency dips [7, 8]. When a large amount of electricity from the grid is generated utilising renewable energy sources with a high degree of variability, such as wind, solar, and wave/tide, this support may become critical.

1.1.1 MVDC Networks

In addition to networks of AC distribution, MVDC networks are now seen as a promising latest technology for enhancing power quality and transfer capacity in distribution systems. These technologies have a few benefits as compared to AC grid systems. The capacity of electricity transmission can be increased because no reactive current is transferred in MVDC distribution networks. Furthermore, MVDC uses fewer materials and eliminates the disadvantage of having to build large power conversion equipment like transformers. Low currents at medium voltage result in fewer conduction losses in these systems. [5,6]. The increased interest in MVDC systems is due to the expansion of the energy market, which has resulted in the installation of a large number power plants. The present rate of adoption of these technologies will need the creation of a dc integration connection, which can be accomplished utilising MVDC networks [7]. MVDC systems have become the subject of both practical and theoretical research as a result of these advantages [8,9].

According to [10], the majority of the loads serviced by AC power systems are of the DC type. Because about 80% of business and residential loads are DC [11], including medium voltage DC networks into power supply systems can decrease DC-AC-DC conversion losses, resulting in reduced circuit energy consumption. The integration of EVs with MVDC networks in this thesis model can help the EV model reduce these losses. Current EV charging stations rely on AC chargers, which necessitate a two-stage AC-DC-AC conversion procedure on the transmitting side. A rectifier converts the low frequency AC supply to DC, which is subsequently converted to AC with a high frequency using an inverter since the resonant circuit demands high frequencies. Apart from the advantages described above, MVDC networks can avoid the two-stage conversion process in electric vehicles, therefore having EV systems directly connected to the MVDC architecture can improve system efficiency by reducing the number of power conversion stages.

1.2 LITERATURE SURVEY AND BACKGROUND RESEARCH

1.2.1 WPT Technologies

Nikola Tesla was the first to introduce WPT, doing different tests on it at Colorado Springs, USA in the 1890s [12]. WPT uses an air medium that is electrified

by charged particles to transport energy between the transmitter and receiver. Energy can be conveyed by an electric field, a magnetic field, or electromagnetic waves, depending on the uses, power ratings, and transmission range. WPT techniques are classified into near field and far field based on distance, as shown in Fig 1.1. Near field approaches are utilised when transferring energy over short distances; far field methods are employed when transferring energy over large distances.

Microwave beamforming, one of the far field technique's approaches, has recently been applied in EVs and PHEVs. In [13], a device was developed that uses an 80 percent RF-DC conversion efficiency roadside the transmitter to power the EV. This approach has been employed in the applications related to medium power, such as recharging portable electronic gadgets, for the past ten years. Far field technologies, on the other hand, use stronger electromagnetic fields than near field technologies, making near field transmission safer for people [14-16]. As a result, the design of this system model uses the Inductive power transfer (IPT) method in WPT, which is classified as near field transmission. Despite the constraints of near field systems in terms of transmission range, lower data rates, and sensitivity in relation to the transmitter and receiver positions, these variables may not impair performance in existing applications that only require low data rates over short distances. According to some academics, these technologies can also be beneficial in terms of achieving security [17].
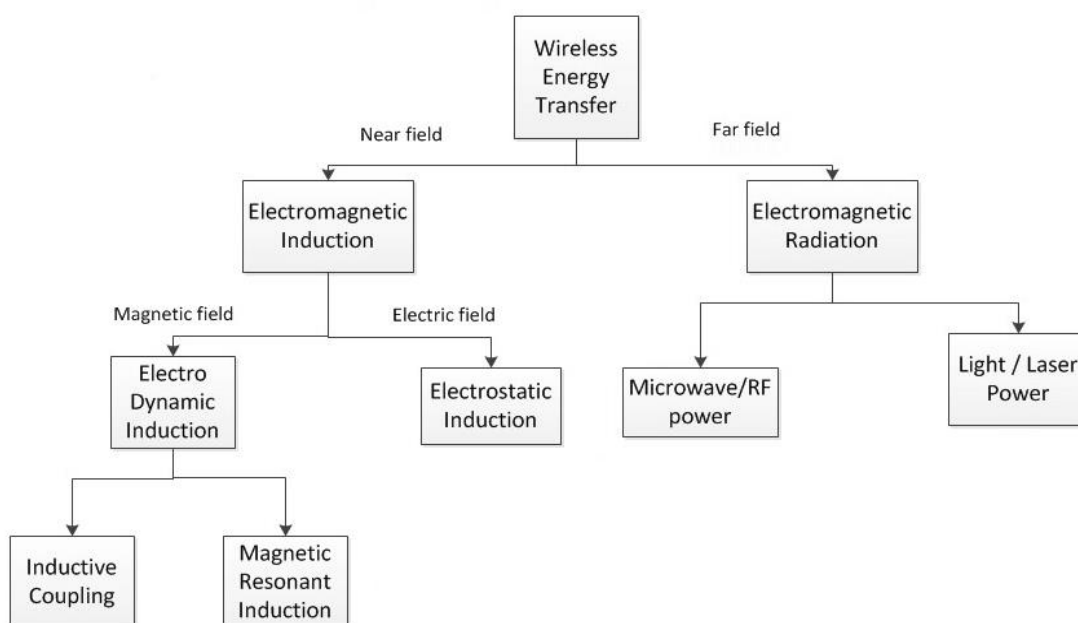
Fig 1.2 Energy transfer examples in near and far field

WPT is now employed in most mobile devices, electric vehicles, and home appliances [18] because to its advantages. Solar power satellites and defence systems also use it.

1.2.2 Inductive power transfer

There are two main strategies for near-field transmission that are now being employed in real applications and can be classified depending on the coupling technology used in them. The strategies for coupling are mentioned as follows.

- Inductive coupling
- Capacitive coupling

Inductive coupling is a near-field transmission technology in which energy is transferred between two coils by means of magnetic fields. For transmission from transmitter to receiver, the coils will be arranged near together. Without using any physical channel, the mutual induction principle is employed to transfer energy between the two coils. When a current is passed via the transmitter coil, it produces a short-range magnetic field. The current or voltage will be induced in the receiver coil when it is brought and positioned in this field. This induced voltage can be utilised to power a wireless device or a storage system. The magnetic field is used to transfer electrical power from one coil to the other coil in this fashion. Energy will be transmitted between the coils in inductive coupling due to mutual induction. Figure 1.2 depicts the fundamentals of inductive coupling. A transformer can be a good example of how mutual induction works because the primary and secondary coils do not come into touch.

Inductive power transfer can manage a wide range of power loads without serious issues and with higher efficiency, and it is employed in a wide range of near-field applications since it can maintain higher efficiency within a metre [19]. The mutual position and distance of the transmitter and receiver are factors in determining transmission accuracy. However, this strategy is only effective across short distances. The quantity of power transfer is reduced if the distance between the coils is increased or the secondary coil is separated from the primary coil. The use of inductive coupling for longer-distance power transmission is still under development [20]. Capacitive

coupling, like inductive coupling, is generally utilised for short distances, but the power is transferred through electric fields.
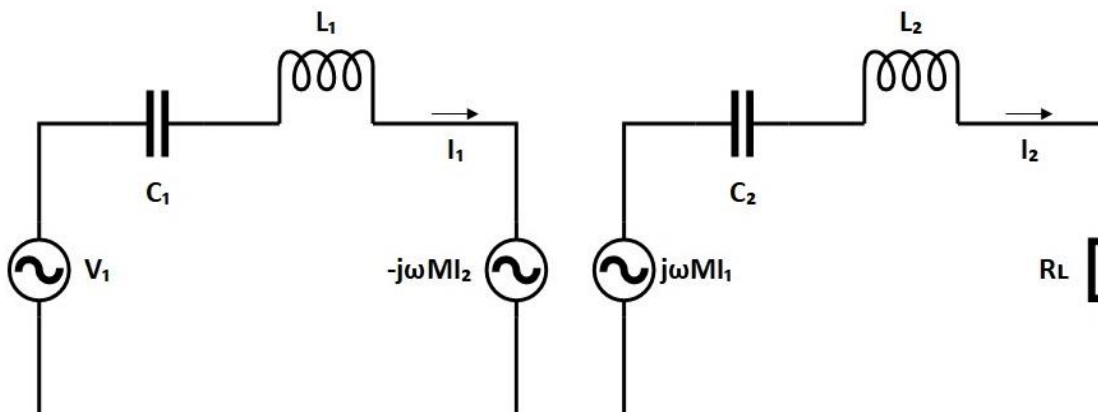

Fig 1.2 Inductive coupling

Despite the fact that both of these coupling strategies can be utilised for power transfer in EVs, this model prefers inductive coupling over capacitive coupling due to its advantages. Inductive coupling has a number of advantages over capacitive coupling as listed below:

1) Although CPT is gaining popularity in small-gap applications, it is confined to low-power transmissions over short distances, whereas IPT can handle both low- and high-power transmissions. CPT is used in applications that require power transmission in centimetres, such as EVs, factories, and industrial automotive applications, whereas IPT is used in applications that require power transfer in centimetres. [20]
2) IPT is less dangerous than CPT since it transfers electricity using magnetic fields rather than electric fields.
3) IPT can operate at frequencies ranging from 10 kHz to 10 MHz, whereas CPT can operate at frequencies ranging from 100 kHz to 10 MHz.

There are several more significant benefits to use the IPT approach in this system:

1) **Friendly to environment**: Because it includes two individually contained sections, IPT can work in severe situations. Dirt, dust, and chemicals have little effect on it. It doesn't leave behind any carbon leftovers that could be hazardous to the environment. The magnetic effect on humans is one of the issues that was discussed in IPT. However, study conducted at the University of Auckland's medical school demonstrates that there are no detectable detrimental biological

impacts at low frequency ranges [21]. Unlike radio frequencies, these low frequencies normally do not have enough power density to heat human body cells.

2) **Robustness and Reliability:** Because there is no direct friction in these systems, there is no electrical erosion or wear and tear. Because the electrical components of this system are totally closed, there is no chemical degradation in the conductor portions. As a result, there is less upkeep necessary.

Despite the numerous benefits associated with IPT, there are a few drawbacks. These systems' power levels are insufficient for industrial usage. Strong coupling between the transmitter and receiver is not an option for IPT. Because of the loose coupling, they are nearly impossible to use in high-power applications. Misalignment in coil placement may also have an impact on the IPT system's performance. According to [22], when the coils are misaligned by 25%, efficiency drops to 92 percent. IPT alone cannot be utilised to construct EV systems because of these flaws. To address IPT's shortcomings, this system incorporates resonant systems into the IPT system, that may aid IPT in improving system performance. The following chapter will go over the features and benefits of implementing these resonant circuits.

1.2.3 Batteries for Electric Vehicles

Despite the benefits of electric vehicles, technological limitations such as higher costs than equivalently sized gasoline engines, long charging periods, limited battery life, and limited travel distance on a single charge remain [9]. One of the most important components to research and develop in order to break through the barrier is the battery.

The most significant elements to consider when purchasing an electric vehicle battery are safety, power density (power, volume, and weight), cost, reliability, and lifetime. First and foremost, the EV prioritises safety [10]. Over-voltage, over-current, deep discharge, over-temperature, and cell charge balance are all critical safeguards. Second, because electric vehicles have limited room, power density is a more pressing concern. The range of an electric vehicle is determined by the amount of energy stored in its battery, which is measured in amp-hours (Ah). The power rating of the battery, which is indicated in watts, determines the rate of charging and discharging (W). Finally, there are two techniques to evaluate the battery life span: minimum calendar life and total charging/discharging cycle life [11]. With a certain capacity, a vehicle battery is

projected to last 10-15 years [12]. While trade-offs must be addressed, an EV battery should be able to achieve all of these requirements at a fair price, as the high cost of batteries has previously been a significant barrier to widespread adoption of electric vehicles [13].

Lead-acid batteries, nickel metal hydride (NiMH) batteries, and lithium-ion (Li-ion) batteries are the three main battery technologies now used in EVs, with their key attributes shown in Table 1.1 [14].

Table 1 Electric vehicles Batteries comparison

Battery Type	Cost	Energy density	Capacity of Power discharge	Rate of Self-discharge	Life span
Lead-acid	Inexpensive	Low	Good	High	Short
NiMH	High	High	Good	High	Long
Li-ion	Reasonable	High	Good	Low	Long

The lead-acid battery that powered early electric vehicles like the GM EV1 [15, 16]. It has a high discharge power capacity that allows it to respond quickly to load fluctuations. Meanwhile, due to the technology's advanced development, the price is reasonable. However, it is not ideal for the current EVs due to its low energy density, heavy-weight, and limited life period due to deep discharging degeneration.

Toyota Prius [17] and Honda Insight [18] both use NiMH batteries. A NiMH battery offers a higher power density than a lead-acid battery because the charger/discharge operations are simpler. The EV with a NiMH battery has twice the driving range as the comparable lead-acid battery due to the high-density feature [19]. A NiMH battery also has a longer life cycle since it can withstand moderate overcharges and severe discharges. Because the NiMH battery has a low internal resistance and a significantly higher charge acceptance capability, the charging efficiency is higher. The biggest downside of NiMH is its rapid self-discharge rate, which means that while the battery is not in use, it will lose charge. It also has a higher cost and a lower charge acceptance capability in high temperatures, lowering charging efficiency.

For newer generations of EVs, such as the Nissan Leaf [20, 21], lithium-ion (Li-ion) batteries have become one of the preferred energy storage units. Although the Li-ion battery has issues that need to be addressed, such as cell life, cell balance, cooling operation, cost, and safety, it has the advantages of higher energy density, higher power rating (high cell voltage and output power), lower weight, and greater discharging power for faster acceleration when compared to other rechargeable batteries. The following are some of the advantages [12, 22-25]:

1) One of the most appealing features is the higher power density. Li-ion batteries are substantially lighter than other types of batteries when it comes to providing the same level of capacity. For example, the AC Delco lead-acid battery pack in the Chevrolet Volt weighs 590 kg to provide the same amount of energy (16kWh), whereas the new Li-ion battery pack weighs only 170 kg, or 28.81 percent less than the original option.

2) Lithium-ion cells have a self-discharge rate of 2 to 3 percent per month, which is substantially lower than Lead Acid (4 to 6 percent per month) and NiMH (30 percent per month). As a result, the Lithium-ion battery has a substantially longer life expectancy than other types of batteries. Furthermore, the Lithium-ion battery's discharge curve is fairly flat. It is commonly understood that if the battery's power output drops rapidly during the discharge cycle, a dangerous issue can arise towards the end of the cycle, especially for high-power applications. The Lithium-ion battery, as illustrated in Fig. 1.3, offers essentially constant voltage (corresponding stable power) for about 80% of the discharge cycle.

3) The inside of a Li-ion battery pack has a high number of cells [26]. The 196 cells in the Nissan Leaf battery pack, for example, are made up of 48 modules, each with four cells [27, 28]. The charging process is faster and more efficient with this arrangement.
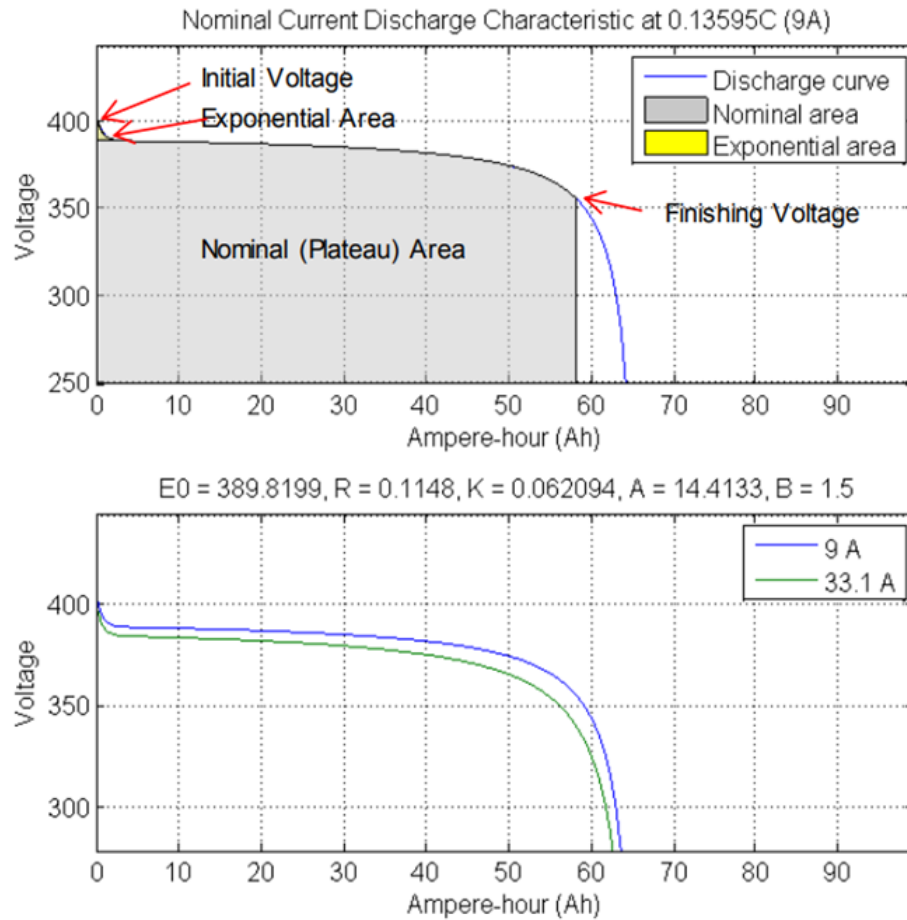
Fig 1.3 The Li-ion battery discharge characteristics [24,30]

1.2.4 Technology for Battery charging

Battery performance is influenced by charging and discharging regulation, as well as battery architecture. As a result, battery charge and discharge control and operation are essential technologies in the entire electric vehicle system [29].

1.2.4.1 Charging approach

Other charging methods include constant current (CC) [30], constant voltage (CV) [31], constant power, taper current, and others [32]. The most basic method of charging a battery is with a constant voltage charger. It operates by supplying the proper current to keep the battery voltage constant. An additional circuit is required to protect the battery. The battery voltage climbs linearly over time when a constant current charger puts a fixed current into the battery (usually the maximum current for fast

charging). For big and expensive batteries, a constant power charger is typically utilised in a slow charging strategy. The most important constraint when charging in a home is the maximum current, which must be less than the single-phase outlet fuses current.

1.2.4.2 Levels of power charging

Level 1 for slow (domestic) charging, Level 2 for primary charging, and Level 3 for fast charging (usually using DC voltage) [9], as indicated in Table 1.2, are the three categories [36, 37] based on different power ratings and charging times.

Table 2 Power levels charging comparison [36, 38]

Type	Classification	Voltage	Power level	Charging time
Level 1	Slow charging	120V @ AC	2 kW	10-12 Hours
Level 2	Primary charging	240V @ AC	19.2 kW	4 Hours
Level 3	DC fast charging	200V-800V @ DC	50kW- 120kW	Less than 1 hour

Level 1 charging is the most basic EV charging level. It is powered by a typical 120 V household socket and has a range of 4 to 5 miles after an hour of charging. Because most EV manufacturers include a Level 1 EVSE wire set, no additional charging hardware is necessary. Recharging a completely depleted EV battery takes about 20 hours [3]. The use of a 220 V inventory framework is mostly limited to North, South, and Central America, Europe, and a big section of the world. This type of charging mechanism requires an installation cost of around 500-880 USD.

Level 2 charging equipment uses a private 220 V supply system or a 208 V charging station outside [3]. In an hour of charging, a 3.3 KW on-board charger can provide roughly 15 miles of travel. A 6.6 KW on-board charger, on the other hand, may travel 30 miles in the same amount of time as it takes to charge. Level 2 EVSEs employ equipment specifically designed to speed up recharging and require skilled electrical installation using a dedicated electrical line. The Level 2 charging system will cost between 1000 and 3000 dollars to set up.

A 480 V AC supply system is required for Level 3 charging. This type of charger may travel 80-100 miles in 20-30 minutes after charging. The DCFC converts AC power

to DC, which is then transmitted straight to the EV battery pack. This level of billing is only appropriate for commercial use, not domestic. The cost of execution ranges from 30000 to 160000 USD.

1.2.4.3 Off- board and On-board charger

Battery chargers for electric vehicles are often divided into on-board and off-board categories, as indicated in Table 1.3. Off-board chargers, also known as standalone fast-charging stations, function similarly to filling stations for liquid fuel vehicles, providing high-power charging at a rapid rate [9]. Off-board recharge stations, which can considerably expand the range of pure-battery EVs, are typically built-in public areas such as shopping malls, car parks, and highway facilities [42]. The size, weight, and space constraints for developing such an off-board station are lessened; however, these stations require large investment and long-term development time.

On-board chargers, on the other hand, are incorporated into the vehicles and provide 6-16 hours of charging time at 2-20 kW of power [9]. On-board chargers make it simple to charge electric vehicles overnight when they are connected to a residential utility socket. The charger will be less expensive than an off-board charger station because it may be incorporated within the vehicle. Despite the fact that the input power level is limited by size, weight, and space constraints, making charging slow, on-board charging remains a viable option due to its compact size, convenience of use, and low cost. The conductive method and inductive approach, both of which rely on direct electrical contact between the grid and the on-board charger, are available.

Table 3 Comparison of off-board and on-board charger

Classification	Size limit	Weight limit	Space limit	Construction requirement	Power rating	Level type	Charging time
Off-Board	less	Less	Less	Yes	50kW	3	Fast charging less than 1 hr
On-board	Yes	Yes	Yes	Less	2-20kW	1,2	Slow charging 4-12 hrs

On-board chargers normally use Level 1 and Level 2, which are intended to be fitted in the vehicle, according to the SAE J1772 standard [26], whereas off-board chargers typically use Level 3.

1.2.5 Design requirement of EV battery charger

The onboard charger which typically consists of two stages, front end pfc and dc-dc converter. The prime objective while designing an onboard charger is:

- Unity power factor for better power quality

- Zero voltage switching leading to High efficiency

- Reduction in size and weight of the charger

- High power density

- Isolation at the output end for enhanced safety

1.2.5.1 Power Quality

The full-bridge rectifier present on the input side of the converter makes the input current at the converter end out of phase from the source voltage resulting in poor power quality. The converter operating in a discontinuous mode often reduces the power quality at the input side of the source which needs to be improved as per IEEE standards and regulations enforced by various power supply units. A way to improve the power quality is by using a power factor correction circuit.

1.2.5.2 High efficiency

Major losses are categorized as switching losses and conduction losses. At high-frequency operation, the switching losses predominate the conduction losses. To reduce the switching losses at the high frequency, the primary switch is turned on/off at zero voltage (ZVS) and/or zero current (ZCS) condition avoiding any switching losses. With the advent of Silicon carbide and Gallium nitride technology, $R_{ds(on)}$ of the primary switches are reduced considerably which ultimately could reduce the conduction losses. Another approach to reducing the conduction losses is to replace the diodes at the rectifier with Mosfet, commonly known as synchronous switching. Through ZVS/ZCS

switching losses can be avoided and through synchronous rectification conduction losses can be avoided resulting in high efficiency across the converter operation.

1.3 OBJECTIVE OF THE THESIS

The goal of this thesis is to build, model, and analyse a 2KW Resonant Inductive Wireless power transfer system for electric vehicles (EVs) in order to connect them with MVDC networks, with benefits such as improved system performance over standard EV systems. This thesis' system is suitable for commercial electric car applications. Despite the fact that many existing EV systems are connected to the AC grid, this proposal connects EVs to MVDC systems.

Resonant circuits can be added into WPT systems with IPT to address the shortcomings of IPT. The supply frequency is made equal to the circuit resonant frequency in a resonant circuit, and the system performs well when it is at resonance. This model system takes advantage of this advantage and seeks to create a system that performs better. The primary circuit is tested in MATLAB/Simulink software. After generating the equations for each component, the values of the components are calculated. To ensure that the designed model is viable, these calculations are compared to simulation findings.

1.4 OUTLINE OF THE THESIS

The first chapter presents electric vehicles (EVs), MVDC networks and their benefits, and EV-MVDC network integration. It underlines the benefits of utilising WPT in EVs. It looks at how existing WPT methods in EVs can be improved by employing resonant systems in this thesis model, as well as how existing IPT methods in EVs can be improved by using resonant systems.

The characteristics of resonant inductive power transfer are discussed in Chapter 2. It discusses the design strategy for a 2KW WPT system used in this thesis. It delves into the block diagram and components such as the PWM Module, which houses the controller and driver circuits, as well as the role they play in the system's design. It also goes through the power conversion step of the inverter and the resonant circuits used in the design.

The chapter 3 presents the coil design for wireless power transmission system, designing of coupling coils, selection of the coil geometries, and the material selection for coil designing.

The basic circuit model's simulation design and analysis are described in Chapter 4. It depicts the derivation and theoretical calculations of the model's primary circuit components. The system's analysis and simulation findings are thoroughly analysed.

Chapter 5 closes by describing how to verify the developed system for practical applications.

CHAPTER 2

WIRELESS POWER TRANSMISSION SYSTEM

2.1 RESONANT INDUCTIVE WPT

Tesla was one of the first to work on merging WPT with resonance, explaining the benefits of tuning the transmitting and receiving coils at resonance frequency, that is similar to the concept of an oscillation transformer. The key premise behind the integration of resonance with WPT [23, 24] is the oscillation transformer. Resonant circuits are used in conjunction with the IPT in order to improve the coupling and performance of the IPT system, as explained in Chapter 1. The use of resonant circuits can extend the transmission range of IPT devices. To obtain the resonance frequency, resonant circuits are used, which can improve the rate of energy transfer. An inductor and a capacitor are used to make a resonator. Magnetic resonance coupling is a technology that combines inductive coupling and resonance. Magnetic resonance coupling allows for very strong interactions between two objects [25-28]. Energy may be transmitted from the source to the receiver very efficiently and with very little energy waste with this technology. When compared to the standard IPT [29], it is highly efficient, with minimum radiation losses and excellent range and directionality.

Magnetic resonance coupling is resistant to the surrounding environment because of its resonance feature. If the primary and secondary coils are misaligned in an IPT system without resonance, the power transmission between the transmitter and receiver can be reduced, while resonant circuits can provide flexibility in the source and load orientation during operation [30, 31]. Magnetic resonance coupling has the added benefit of being able to be used between a single transmitter and a large number of receivers. It is capable of transmitting electricity even when the power requirements of various load devices differ. This technology is at the forefront of research, and it is being used in electric vehicles (EVs), consumer electronics, medicinal implants, wireless sensor networks, and robotics power supplies as a result of its advantages.

Electrical resonance occurs in an electric circuit when the imaginary parts of the impedances or admittances of the circuit elements cancel each other out at a specific frequency known as the resonant frequency. At this specific resonant frequency, a circuit's response is maximised. Resonance can arise in any circuit with an inductor and

a capacitor, as both of these components can store energy [32]. The energy oscillates between the inductor and the capacitor in a resonant circuit, and the rate at which the energy is transferred between these two elements is determined by the values of L and C. We will notice oscillations in the circuit as a result of these energy transfer oscillations. These oscillations will continue indefinitely if this circuit is perfect and no resistant elements are present. In actuality, all of the circuits will have some resistance. These oscillations will depreciate as a result of the presence of this resistance. To keep these oscillations going, we'll need to feed this LC circuit power from an external source with the same frequency (which was addressed as resonant frequency). We can keep the oscillations going this way. The two primary basic resonance circuits are parallel and series RLC circuits. Quality factor is a term used in resonance circuits to describe the sharpness of the resonance. The formula below calculates the Quality factor.

$$Q = \frac{Stored\ maximum\ energy\ in\ the\ circuit}{Energy\ dissipated\ by\ the\ circuit\ in\ one\ period\ at\ resonance}$$

This Quality factor is given by the equation below in a series resonant circuit.

$$Q = \frac{\omega_o L}{R} = \frac{1}{\omega_o C R} = \frac{1}{R}\sqrt{\frac{L}{C}} \qquad (2.1)$$

Whereas in a parallel resonant circuit, it is given by following equation.

$$Q = \frac{R}{\omega_o L} = \omega_o R C = R\sqrt{\frac{C}{L}} \qquad (2.2)$$

The equations for the main circuit model employed in this system model, which will be explored in the next chapter, are obtained utilising these principles of basic resonance circuits. Resonant circuits also have the advantage of being able to enhance voltage and current levels based on their topology, which makes them excellent for IPT applications. A voltage amplifier can be created using a series resonant circuit, and a current amplifier can be created using a parallel resonant circuit. When the circuit is used as a voltage amplifier, the voltage produced at the resonant circuit is much higher than the supply voltage.

The voltage across the inductor in a series circuit at resonance can be calculated using equation 2.3.

$$V_L = \frac{Vm}{R} = \omega_o L \qquad (2.3)$$

We know that, $\frac{\omega_o L}{R}$. is the Quality factor Q, therefore if we replace that term with Q in the above equation, we get equation 2.4.

$$V_L = VmQ \qquad (2.4)$$

The voltage across the inductor will be significantly bigger than the input supply voltage, as shown in the above equation; thus, this circuit can operate as a voltage amplifier. The similar approach may be used to the voltage across the capacitor, allowing us to obtain greater voltages at higher frequencies by carefully setting the values of L and C in the resonant circuit.

2.2 2 KW WPT SYSTEM

The system design employed in this model is depicted in block diagram form in Figure 2.1. The transmitter and receiver are the core components of any wireless power transmission system. It requires a source of input power, which might be AC or DC.
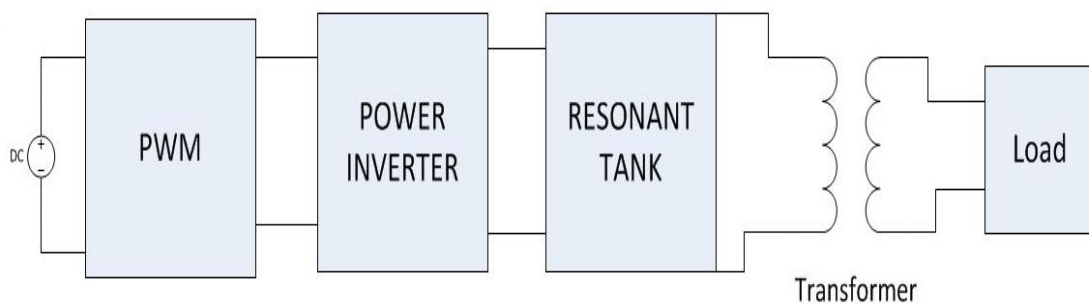

Fig 2.1 2 KW system setup

On the transmitter side, as shown in Fig. 2.1, power electronics converters are employed to convert DC supply to AC at the desired frequency. This is accomplished through the employment of a full bridge inverter topology. A two-stage AC-DC-AC conversion method was employed in several WPT models, as indicated in Chapter 1, although this entire process necessitates circuitry incorporating switching devices. The greater the number of switching devices, the greater the switching losses.

MOSFETs are utilised in the inverter in this model for switching functions. MOSFETs, in general, have two types of losses: conduction and switching losses [35, 36]. Switching losses occur when the switch is turned on and off. The formulas below calculate the switching losses in these switches when they are turned on and off.

$$\text{Power losses during Turn ON: } P_{on} = E_{on} f_{sw} \qquad (2.5)$$

$$\text{Power losses during Turn OFF: } P_{off} = E_{off} f_{sw} \qquad (2.6)$$

where,

The energy dissipated at the switch during ON and OFF are *Eon* and *Eoff*, respectively, while the switching frequency is *fsw*.

The switching losses are directly proportional to the switching frequency, as shown by the two formulas above. Higher frequencies can make the system more compact, however as previously stated, higher frequencies can result in switching losses. It's also important to look into the EMF emissions that high frequencies can cause. Switching losses can be reduced by reducing the number of power conversion stages.

2.2.1 Pulse Width Modulation Module

The system is made up of a PWM module, which is made up of two circuits that generate pulses to operate the inverter's switches. These are the two circuits.:

1) Controller IC
2) Driver circuit

The inverter switches are controlled by the controller by phase shifting the switching of one-half bridge in relation to the other, which allows for constant frequency pulse width modulation. It sends signals to the driver circuit, which serves as a connection between the controller and the switches.

2.2.2 Driver circuit design

MOSFETs have parasitic capacitance as a result of their design. MOSFET switching speeds may be slowed by this parasitic capacitance. The input parasitic capacitance, which is the total of gate source and gate drain capacitance as perceived from the input, must usually be charged in order for the MOSFET to turn on, hence this parameter is critical in real applications. To operate, the parasitic capacitance at the input

must be charged to the MOSFET's minimum gate voltage. To turn the transistor off, this capacitance must be decreased.

When the MOSFET is turned ON or OFF, it may not immediately begin to conduct and may conduct a large amount of current. The gate current that is delivered to a MOSFET to turn it ON can generate a certain amount of heat, which in some situations can harm the MOSFET. Therefore, shortening the switching time may be important to reduce switching losses, but this may require more current to charge the gate. The control signal generated by the microcontroller is restricted to currents of a few milli amperes.

The MOSFET will turn on slowly at this low current, resulting in considerable switching losses. Furthermore, the parasitic capacitance mentioned before may consume a lot of current, potentially harming the hardware. All of this harm might be avoided if gate drivers were used. The gate driver can create a high current input for the MOSFET gate. As a result, switching time and switching losses can be decreased. In this approach, the gate driver safeguards the switches while also acting as an interface between the controller and the power switches.

2.3 CIRCUIT TOPOLOGY

Figure 2.2 depicts the basic circuit diagram for this system architecture. On the transmitting side, we can identify two important sections in the main circuit diagram:
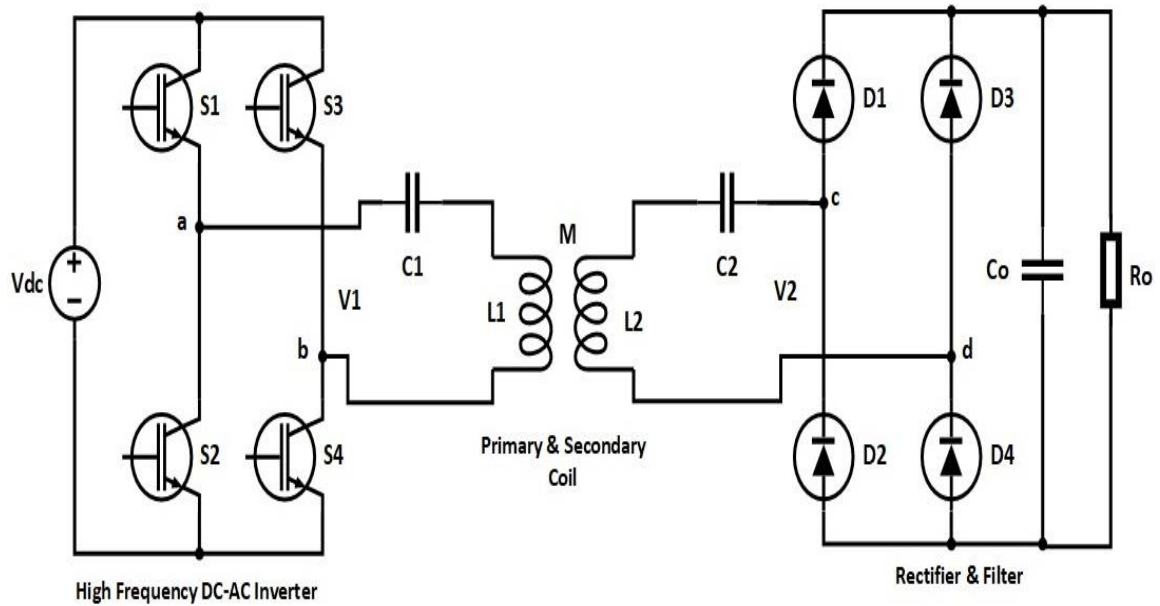
1) Inverter circuit
2) Resonant circuit

Fig 2.2 Major circuit diagram of 2KW proposed system

It is clearly observed from Fig 2.2 that the wireless charging system has two parts, primary/transmitting coil and the secondary/receiving coil. The primary side has DC supply and inverter section and the receiver side has rectifier and load section. The primary is supplied with grid power and its setup is installed at the charging stations/parking area of vehicles, whereas the setup of receiver is installed inside the EVs. The configuration must be operated at the resonating frequency to obtain the maximum power transfer from the primary to secondary coil.

To compensate the losses and to achieve the resonance condition in the primary and secondary coil, capacitor C1 and C2 are used.

2.3.1 Inverter circuit

The planned main circuit's inverter transforms DC to AC and feeds it to the resonant circuit. There are a variety of inverter resonant circuit topologies now in use in actual WPT applications. Several resonant inverter topologies are described in [33], and a few are given below.

1) Class E resonant inverter
2) Class D resonant inverter
3) Class DE resonant inverter

Only one of the inverter's two half bridges will be active at any given time. To achieve the desired output, the switches are performed in parallel. A full bridge inverter can be configured in one of four ways. The several stages of the complete bridge inverter are given in table 2.1 if the input voltage being provided is referred to as Vin.

Table 4 Different stages of full bridge inverter

S1	S2	S3	S4	Vo (Inverter output voltage)
ON	ON	OFF	OFF	Vin
ON	OFF	ON	OFF	Zero
OFF	OFF	ON	ON	-Vin
OFF	ON	OFF	ON	Zero

The output of the inverter based on the varied switching actions of the switches can be deduced from the table above.

2.3.2 Resonant circuit

The capacitor and inductor designated C1 and L1 in Fig. 2.2 are resonant capacitor and inductor, respectively. As previously said, these two components play a significant part in the circuit design since they are critical in producing the resonance condition and boosting the IPT system's performance. These numbers are determined using a few equations that are deduced and described in the following chapter.

The full bridge inverter is employed in this system model because it is a simple and easy-to-build architecture that can produce higher output voltages than other inverter topologies. Despite the limited transmission range, inductive coupling can have a high charging power when the transmission distance is shorter than the coil diameter. However, resonant systems are used to improve transferring ability, and it has been proved that employing magnetic resonant systems can improve inductive power transfer system performance by up to 90% when the transmission distance is up to a metre [34]. The performance of this system model can be improved by combining these various modules with the benefits listed.

CHAPTER 3

COIL DESIGN FOR WIRELESS POWER TRANSMISSION

3.1 DESIGN OF COUPLING COILS

Magnetic resonance coupling consists of two coils that are transmitting and receiving coils. Magnetic resonance coupling works by transmitting power between two coils working at same resonant frequency using a high-frequency alternating magnetic field. The coils could be loosely connected, but energy transmission for several centimetres requires a high Q factor.
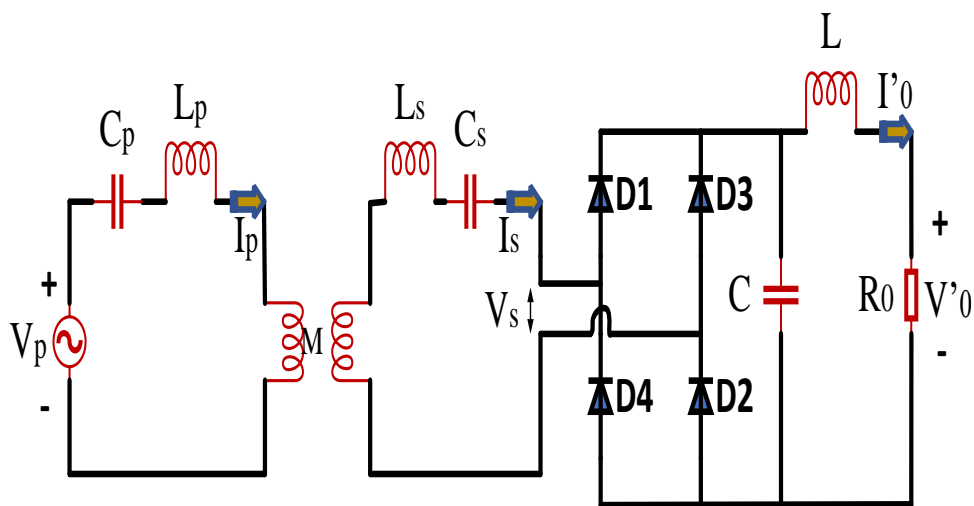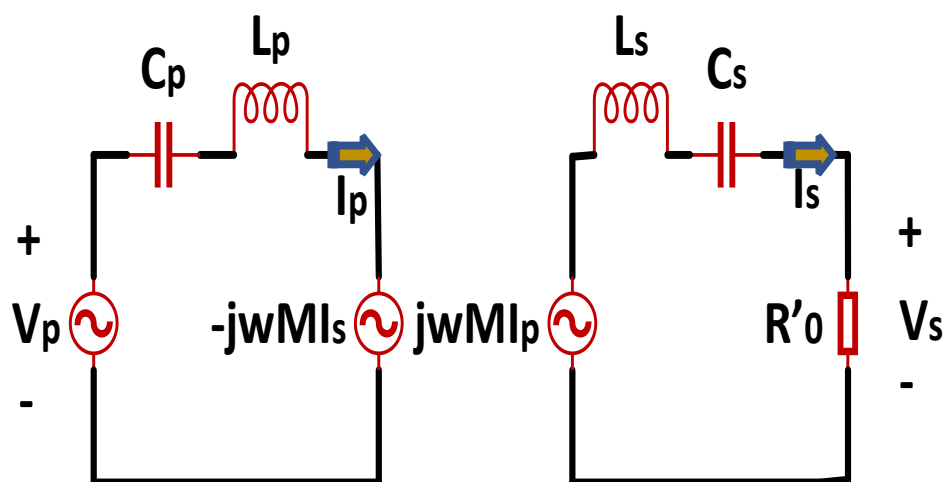

Fig. 3.1 Block diagram of MRC

Fig. 3.2 Magnetic Resonance Coupling

$$Z_pI_p - jwMI_s = V_P \tag{3.1}$$

$$Z_sI_s = jwI_p \tag{3.2}$$

where, Vp is voltage at transmitting Coil, Ip is current through transmitting Coil, M mutual inductance exists between the two coils, the voltage received at receiving coil is denoted by Vs, Is is the current through receiving coil, Ro is the output impedance, R'o is equivalent output impedance.

$$Z_p = jwL_p + \frac{1}{jwC_p} \tag{3.3}$$

$$Z_s = jwL_s + \frac{1}{jwC_s} + R'_0 \tag{3.4}$$

$$R_0 = \frac{V'^2_0}{P_0} \tag{3.5}$$

$$R'_0 = \frac{8R_0}{\pi^2} \tag{3.6}$$

LP, CP denote transmitting coil inductance and capacitance linked in series with coils, respectively, and LS, CS denote receiving coil inductance and capacitance series connected with receiving coil.

Multiplying eq. (3.1) by Zs and eq. (3.2) by jωM

$$Z_pZ_sI_p - jwMZ_sI_s = V_pZ_s \tag{3.7}$$

$$jwMZ_sI_s + w^2M^2I_p = 0 \tag{3.8}$$

Adding eq. (3.7) and eq. (3.8) and dividing it by Zs we get

$$Z_p + \frac{w^2M^2}{Z_s} = \frac{V_p}{I_p} \tag{3.9}$$

$$Z_r = \frac{w^2M^2}{Z_s} = \frac{w^2M^2}{jwL_s + \dfrac{1}{jwC_s} + R'_0} \tag{3.10}$$

Where, Zr is reflected impedance of receiving coil side to transmitting coil side and

$Z_{in} = \dfrac{V_p}{I_p}$ is the impedance as viewed from transmitting coil side.

At resonance frequency (ω_o), the inductor's inductive reactance equals to capacitive's capacitive reactance.

$$jw_0L_s - \frac{j}{w_0C_s} = 0 \tag{3.11}$$

$$C_s = \frac{1}{L_sw_0^2} \tag{3.12}$$

$$Z_r = \frac{w_0^2M^2}{R'_0} \tag{3.13}$$

$$Z_{in} = jw_0L_p + \frac{1}{jw_0C_p} + \frac{w_0^2M^2}{R'_0} \tag{3.14}$$

The imaginary component of input impedance becomes zero at resonance frequency.

$$C_p = \frac{1}{L_pw_0^2} \tag{3.15}$$

The receiving coil sides circuit becomes pure resistive in resonance, the reactance parameters neutralize one another and the, one may obtain

$$M = I_{srms}\frac{R'_0}{W_0\,I_{prms}} \tag{3.16}$$

where, I_{prms} and I_{srms} are the transmitting and receiving coil RMS current.

$$L_s = \frac{Q_LR'_0}{w_0} \tag{3.17}$$

$$K_c = \frac{\sqrt{1 - \dfrac{1}{4Q_L^2}}}{Q_L} \tag{3.18}$$

where, Kc is coefficient of coupling.

$$L_p = \frac{M^2}{L_sK_c^2} \tag{3.19}$$

3.2 SELECTION OF COIL GEOMETRY

The coupling coefficient, which affects the transfer power, has a big impact on the shape and size of the inductance coil. As a result, the shape of the structural parts of the coils structure is crucial.

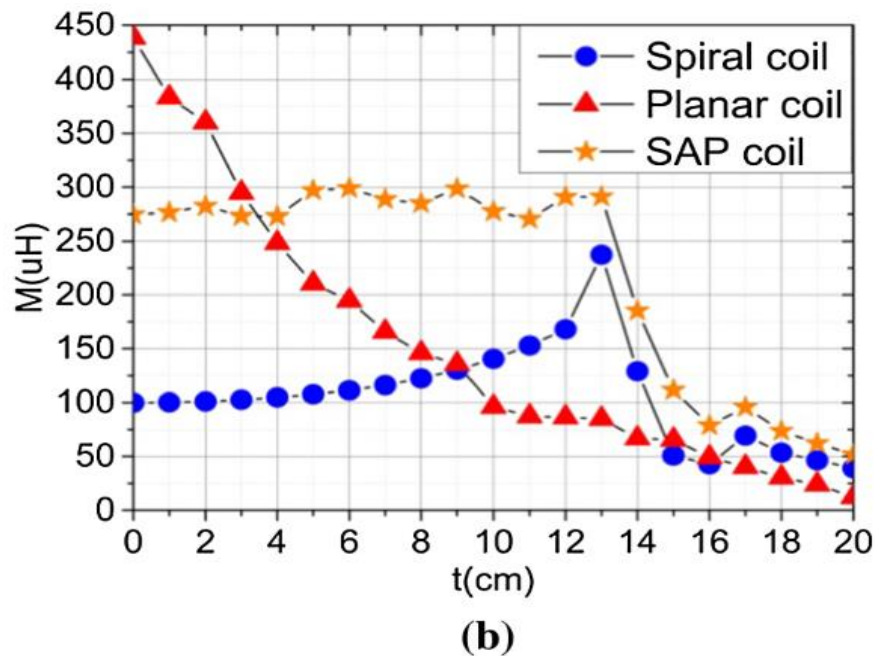IPT inductors come in a variety of forms, including round, square, planar, and rectangular.
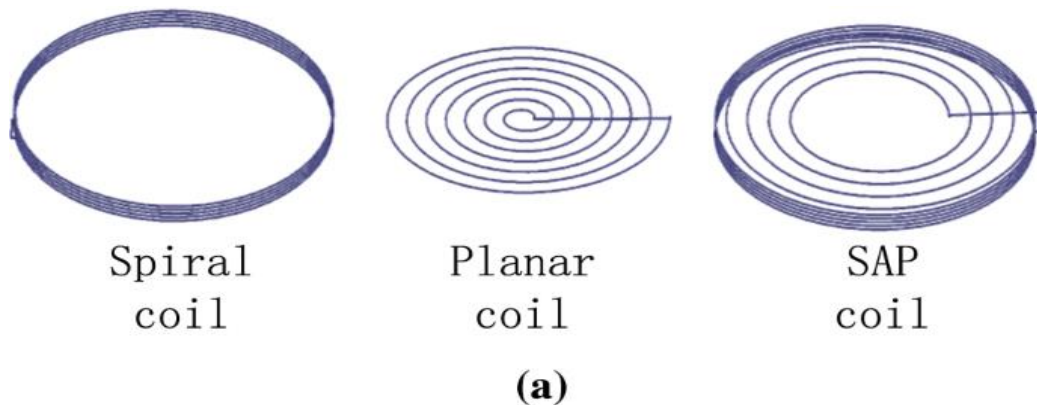

Fig 3.3 Different coil geometries

The highest coupling coefficient is produced by circular and square shapes when their distance between them is adjusted. Because of the more homogeneous field distribution

and uniform geometries in round coils, good results for most similar parameters are achieved. In round coils, copper is used less often.

3.3 MATERIAL SELECTION

There is no solid core inside the coils of an air core inductor. In addition, air cored coils are those that are wound on nonmagnetic materials like ceramic and plastic.

3.3.1 Iron Core Inductor

The number of spires (turns), length, diameter, and thickness of the spiral all affect the inductor inductance value. The range of air core inductance values is limited. An iron core is put within an inductor in order to boost its inductance value. The magnetic properties of this iron core are quite unique. They work to strengthen the magnetic field. When the magnetic field that influences the inductor varies in a continuous way, the bias of "the molecular magnetic domains" determines the magnetism of the core material.

3.3.2 Ferrite Core Inductor

Inductors and transformers use ferrites as one of the main core materials. To raise the inductance of the inductor, a ferrite inductor is utilised to increase the permeability of the medium around the coil. Ferrites are commonly utilised in inductor technology to improve the inductor's performance. Iron-based magnetic materials in the form of ceramics are known as ferrites. Because ferrites are formed from powder, they can be made in a variety of shapes to meet specific needs.

CHAPTER 4

CALCULATIONS AND SIMULATION RESULTS

4.1 EQUATIONS DERIVATION

The theoretical values for the main circuit are calculated using a few equations. On the secondary side of the circuit in the main circuit diagram, there is a load R_L.

The simplified equivalent circuit diagram of the IPT system is designed as illustrated in Fig 4.1 to simplify the calculation. The formulas for designing electrical parameters in IPT topology are examined and obtained using the equivalent circuit shown in Fig 4.1 in this part.
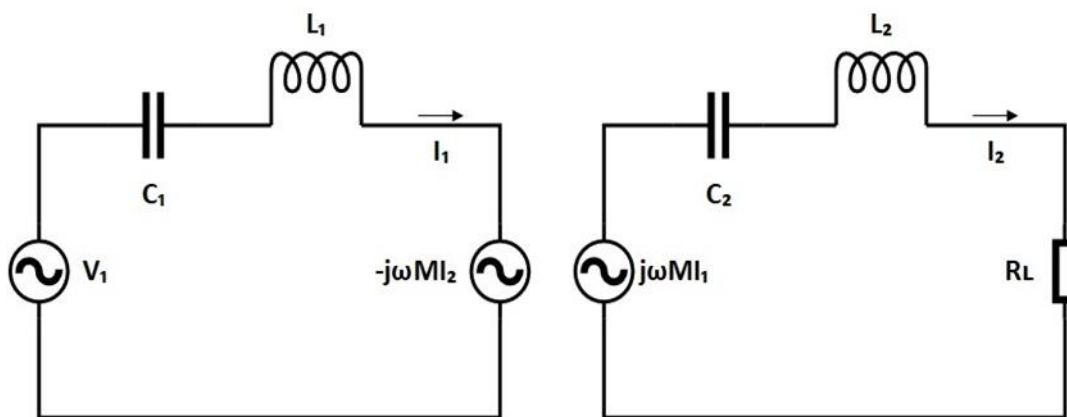

Fig 4.1 Equivalent Circuit Diagram of IPT system

The equations for the main circuit can be determined by following the basic notions of a resonant circuit, as illustrated below.

We know that the imaginary components of the complex impedance or admittance in a circuit are zero at resonance, thus we may solve for the circuit characteristics at resonance by calculating the total impedance and equating the imaginary part to zero.

The self-inductances of primary and secondary coil are shown by L_1 and L_2, C_1 and C_2 are the series compensation capacitances of primary and secondary coil respectively.

From Fig 4.1, in primary and secondary side by applying the Kirchhoff's voltage law in equivalent circuit, one can write

$$Z_1 I_1 - j\omega M I_2 = V_1 \tag{4.1}$$

$$Z_2 I_2 = j\omega M I_2 \tag{4.2}$$

where,

$$Z_1 = j\omega L_1 - \frac{1}{j\omega C_1}$$

$$Z_2 = j\omega L_2 - \frac{1}{j\omega C_2} + R_L$$

Where R_L is the equivalent resistance as seen from the terminals cd in Fig 2.2.

Multiplying Eq. (4.1) with Z_2 and Eq. (4.2) with $j\omega M$, one can write

$$Z_1 Z_2 I_1 - j\omega M Z_2 I_2 = V_1 Z_2 \tag{4.3}$$

$$j\omega M Z_2 I_2 + \omega^2 M^2 I_1 = 0 \tag{4.4}$$

Adding Eq. (4.3) and (4.4), one can write

$$Z_1 Z_2 I_1 + \omega^2 M^2 I_1 = V_1 Z_2 \tag{4.5}$$

Dividing Eq. (4.5) by Z_2, one can write

$$Z_1 I_1 + \frac{\omega^2 M^2 I_1}{Z_2} = V_1$$

$$Z_1 + \frac{\omega^2 M^2}{Z_2} = \frac{V_1}{I_1} \tag{4.6}$$

From Eq. (4.6), (V_1 / I_1) gives the input impedance (Z_{in}) as seen from the primary side of the circuit, and ($\omega^2 M^2 / Z_2$) denotes the reflected impedance (Z_r) of secondary to primary side. Where, Z_r can be expressed as

$$Z_r = \frac{\omega^2 M^2}{\left(j\omega L_2 - \frac{1}{j\omega C_2} + R_L \right)}$$

The reflected impedance Z_r at resonant frequency ω_o can be expressed as

$$Z_r = \frac{\omega_o^2 M^2}{\left(j\omega_o L_2 - \dfrac{1}{j\omega_o C_2} + R_L \right)}$$

The term $j\omega_o L_2 - \dfrac{1}{j\omega_o C_2} = 0$ at resonant frequency, and therefore, the expression for secondary compensation capacitor can be expressed as

$$C_2 = \frac{1}{L_2 \omega_o^2} \tag{4.7}$$

$$Z_r\left(\omega = \omega_o\right) = \frac{\omega_o^2 M^2}{R_L} \tag{4.8}$$

At resonant frequency, the input impedance can be expressed as

$$Z_{in} = j\omega_o L_1 - \frac{j}{\omega_o C_1} + \frac{\omega_o^2 M^2}{R_L}$$

At the resonance condition, the imaginary part of the input impedance becomes zero, and thus, the value of the primary side compensation capacitor can be expressed as

$$C_1 = \frac{1}{L_1 \omega_o^2} \tag{4.9}$$

In the condition of resonance, the circuit of secondary side becomes pure resistive, and the reactance parameters cancel each other, and thus, one can obtain

$$\left| j\omega_o M I_{1rms} \right| = I_{2rms} \times R_L \tag{4.10}$$

From Eq. (4.10), the mutual inductance can be expressed as

$$M = I_{2rms} \times \frac{R_L}{I_{1rms} \times \omega_o} \tag{4.11}$$

Now, the quality factor of the secondary side can be written as

$$Q_2 = \omega_o \times \frac{L_2}{R_L} \tag{4.12}$$

From Eq. (4.12), the design expression for secondary coil inductance can be expressed as

$$L_2 = Q_2 \times \frac{R_L}{\omega_o} \tag{4.13}$$

Also, the coupling coefficient k can be expressed as

$$k = \frac{M}{\sqrt{L_1 L_2}} \tag{4.14}$$

From Eq. (4.14), inductance of primary coil can be expressed as

$$L_1 = \frac{M^2}{k^2 \times L_2} \tag{4.15}$$

When resonance occurs, the angle between the input voltage and current is zero, and the frequency that causes this state is known as resonant frequency or zero power angle (ZPA) frequency. Bifurcation is a phenomenon that occurs in doubly tuned circuits like IPT when, instead of being tuned to a single ZPA frequency, the circuit begins to function at multiple ZPA frequencies. When a circuit parameter, such as the coupling coefficient, is changed, something occurs.

4.2 2 KW CIRCUIT THEORETICAL CALCULATIONS

The equations from the preceding section are used to calculate the circuit. Table 4.1 lists the technical details for the 2 KW system.

Table 5 Parameters of 2 KW system

Parameters	Value
Input Voltage	240 V
Output Power Rating	2 KW
Operating frequency	85 KHz
Quality factor	4
Output Voltage	450 V

Lithium-ion batteries are used in Electric Vehicles which are available in the range of 300-600 V.

Taking output voltage as 450 V and input supply as 240 V, the load resistance will be:

$$Ro = \frac{Vo^2}{Po} = \frac{450 \times 450}{2000} = 101.25 \ \Omega$$

Equivalent resistance as seen from terminals CD in Fig 2.2:

$$R_L = \frac{8}{\pi^2} \times \frac{Vo^2}{Po} = 82 \ \Omega$$

The secondary side rms voltage can be expressed as

$$V2rms = \frac{2\sqrt{2}Vo}{\pi} = \frac{2\sqrt{2} \times 450}{\pi} = 405.35 \ V$$

Self-inductance of secondary side coil is as follows:

$$L2 = Qs \times \frac{R_L}{\omega o} = 4 \times \frac{82}{2\pi \times 85000} = 6.14 \times 10^{-4} H$$

Where, Qs is the Quality factor of secondary side.

I2rms represent the secondary side rms current and can be expressed as

$$I2rms = \frac{V2rms}{R_L} = \frac{405.35}{82} = 4.94 \ A$$

I1rms represent the primary side rms current and can be expressed as

$$I1rms = \frac{Po}{V1rms} = \frac{2000}{240} = 8.33 \ A$$

Mutual Inductance between primary and secondary coil can be expressed as

$$M = I2rms \times \frac{R_L}{I1rms \times \omega o} = 4.94 \times \frac{82}{8.33 \times 2\pi \times 85000} = 9.1 \times 10^{-5} H$$

The coefficient of coupling can be calculated as below:

$$Kc = \frac{1}{Qs} \times \sqrt{1 - \left(\frac{1}{4 \times Qs^2}\right)} = \frac{1}{4} \times \sqrt{1 - \left(\frac{1}{4 \times 4^2}\right)} = 0.248$$

Self-inductance of primary side coil is as follows:

$$L1 = \frac{M^2}{L2 \times Kc^2} = \frac{(9.1 \times 10^{-5})^2}{6.14 \times 10^{-4} \times (0.248)^2} = 219.28 \times 10^{-6} H$$

Series compensation Capacitance of primary side coil can be expressed as

$$C1 = \frac{1}{L1 \times \omega o^2} = \frac{1}{219.28 \times 10^{-6} \times (2\pi \times 85000)^2} = 1.6 \times 10^{-8} F$$

Series compensation Capacitance of secondary side coil can be expressed as

$$C2 = \frac{1}{L2 \times \omega o^2} = \frac{1}{6.14 \times 10^{-4} \times (2\pi \times 85000)^2} = 5.71 \times 10^{-9} F$$

Table 6 Calculated values of 2 KW system

Parameters	Designator	Value
Primary Coil Inductance	L1	219.28 μH
Secondary Coil Inductance	L2	$6.1 \times 10^{-4} H$
Mutual Inductance	M	$9.1 \times 10^{-5} H$
Coupling Coefficient	Kc	0.248
Primary Coil Capacitance	C1	$1.6 \times 10^{-8} F$
Secondary Coil Capacitance	C2	$5.7 \times 10^{-9} F$

4.3 FREQUENCY EFFECT ON CIRCUIT PARAMETERS

The values of resonance frequency or operating frequency can affect the circuit's properties. The increase in frequency, as indicated in the previous chapter, might make the circuit more compact. High frequency ranges, on the other hand, might increase system losses.

The circuit characteristics are calculated for three different frequencies, 30kHz, 50kHz, and 85kHz, to examine the frequency effect theoretically. It has been noted that the values of Inductance and Capacitance have altered with each frequency value.

Below given tables shows the values of L and C for various values of the stated frequencies.

Table 7 L1 and C1 values for different frequencies

Frequency	Value of L_1	Value of C_1
30kHz	$62.19 \times 10^{-5} H$	$4.53 \times 10^{-8} F$
50kHz	$37.56 \times 10^{-5} H$	$2.70 \times 10^{-8} F$
85kHz	$219.28 \times 10^{-6} H$	$1.6 \times 10^{-8} F$

The graphs below show how the L_1 and C_1 values change as the operating frequency changes.

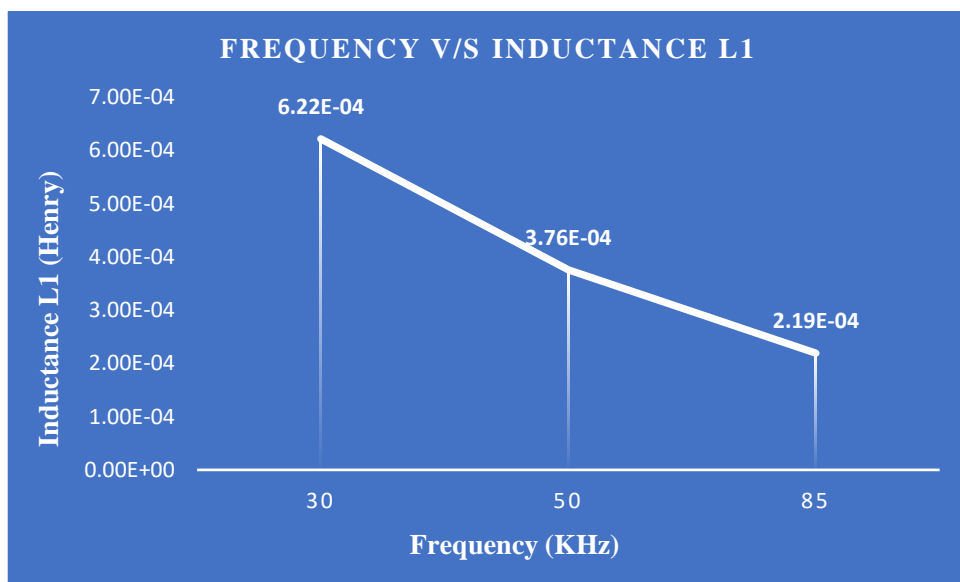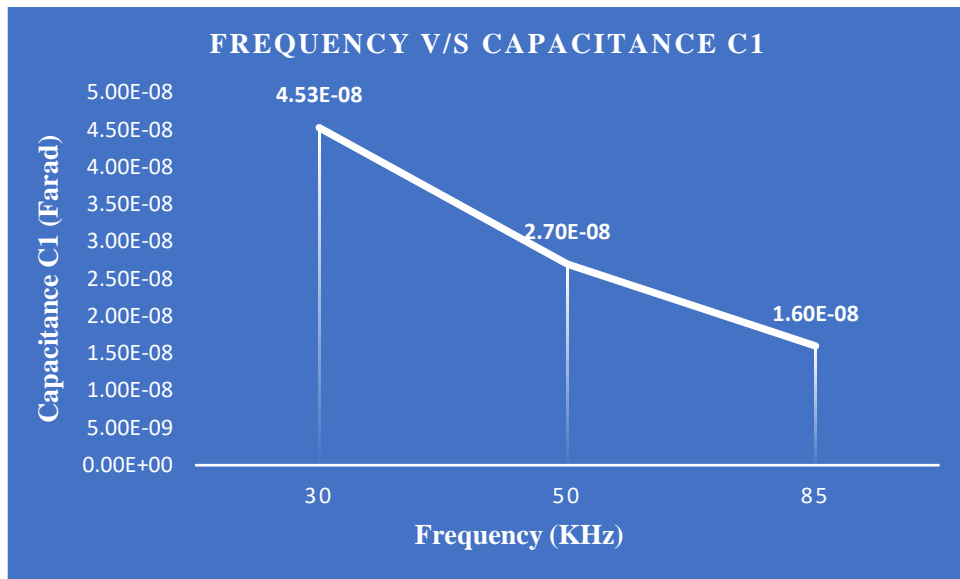Fig 4.2 Frequency v/s Inductance L1 graph

Fig 4.3 Frequency v/s Capacitance C1 graph

Table 8 L2 and C2 values for different frequencies

Frequency	Value of L_2	Value of C_2
30kHz	$1.74 \times 10^{-3} H$	$1.62 \times 10^{-8} F$
50kHz	$1.04 \times 10^{-3} H$	$9.75 \times 10^{-9} F$
85kHz	$6.14 \times 10^{-4} H$	$5.71 \times 10^{-9} F$

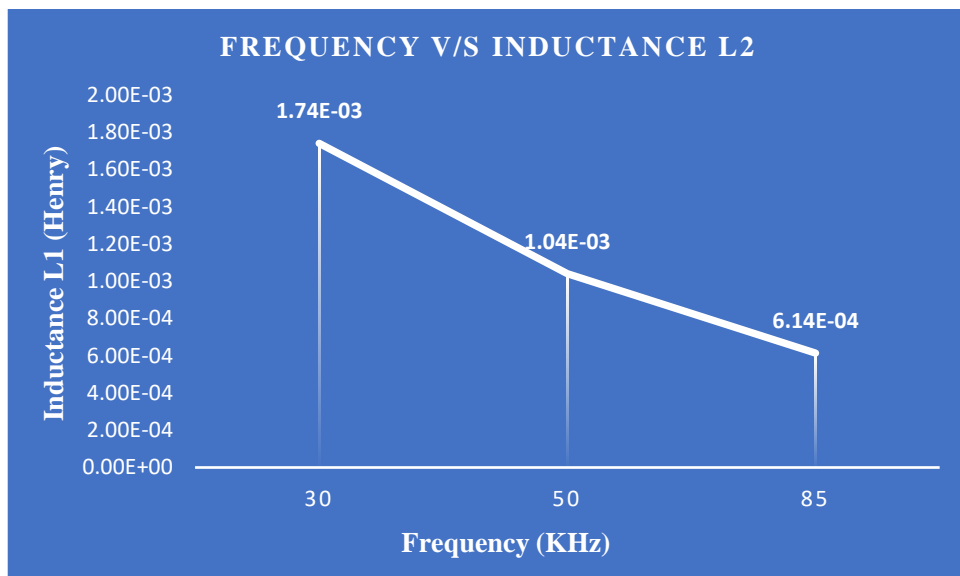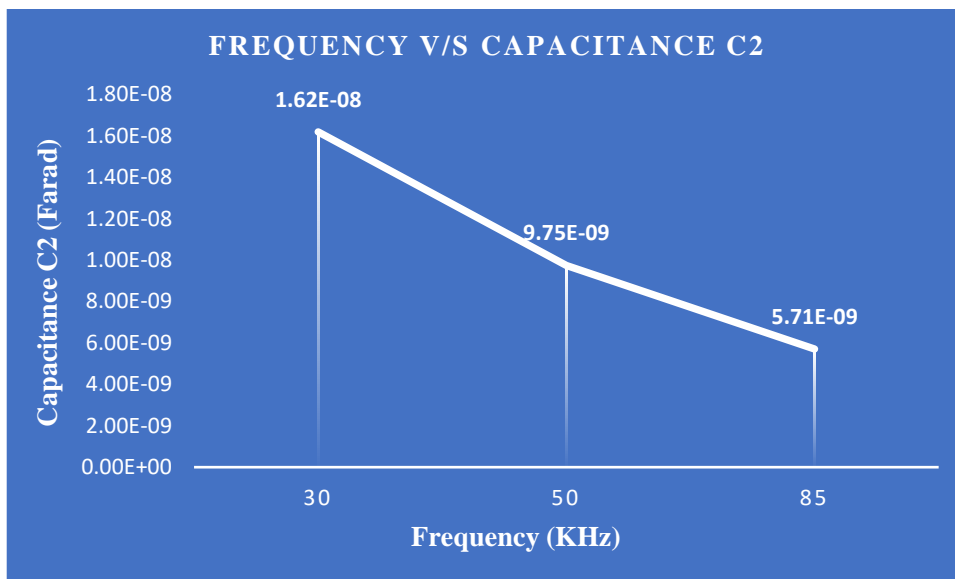The graphs below show how the L_2 and C_2 values change as the operating frequency changes.

Fig 4.4 Frequency v/s Inductance L2 graph

Fig 4.5 Frequency v/s Capacitance C2 graph

From Fig 4.2, Fig 4.3, Fig 4.4 and Fig 4.5, it is clear that the values of inductance L and Capacitance C decreases with the increase in the value of the frequency. This indicates that the system can be constructed with lower value components at higher frequencies, resulting in a smaller system. Because the system becomes bulkier as the frequency decreases, a higher frequency of 85kHz is utilised in this system. Higher frequencies can make the system more compact, but the switching power losses and magnetic field effects must be considered.

To transfer energy from the primary to the secondary side in this system, the coil gets input from the resonant inductor, which it is linked across, resulting in an equal voltage across the inductor and primary windings. Both the Quality factor of the circuit and the voltage across the primary windings fall as the voltage across the inductor is reduced at a fixed output voltage. As a result, the system's ability to transfer enough energy to the secondary side is reduced. This drop in voltage also reduces the distance between the primary and secondary coils over which energy can be transferred, resulting in poor system performance.

4.4 2KW SYSTEM SIMULATION AND RESULTS

The wireless power transmission system as shown in Fig 2.2 was simulated in MATLAB/Simulink as shown in Fig 3.6 with the mentioned/calculated parameters in the above Table 4.1 and Table 4.2. Firstly, the output current, voltage and power are observed with 100 Ω load across capacitor Co without adding Boost Converter on load

side. Again, the output Voltage, Current and Power is observed with 100 Ω load with adding a Boost converter on load side. The output of the designed system can be controlled by the help of Boost converter and by varying the duty cycle, variation in output voltage can be observed.

The gate signals for the inverter are generated using a PWM generator, as shown in the simulation model. The inverter's output feeds the resonant circuit, and energy is transferred from the primary to secondary sides via the inductor coils, which have primary windings connected across the resonant inductor. The results of the preceding sections' calculations are applied to the circuit in the simulation, and the results are compared to theoretical calculations.
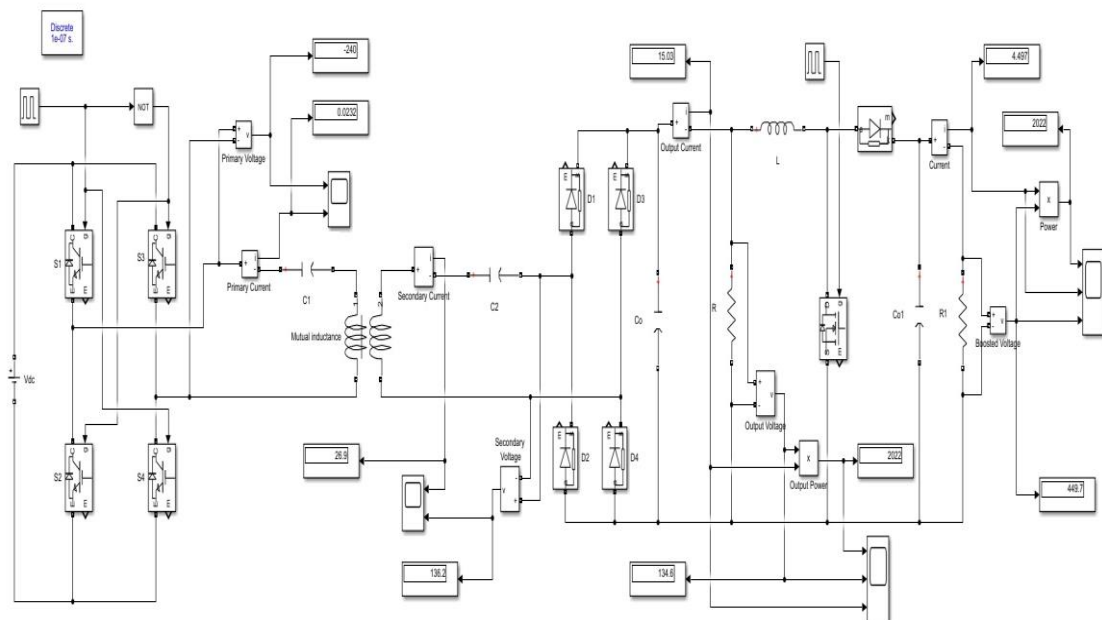

Fig 4.6 MATLAB Simulation of 2KW IPT system

It is observed from Fig 4.6 that the simulation was carried out for transmission of power wirelessly with 240 V dc input supply. This input supply is inverted using high frequency DC-AC inverter then fed to the primary/transmitting coil. By creating resonance between primary and secondary coil, the high frequency AC is supplied to the secondary side by the help of Mutual Induction. The AC obtained from secondary coil is first rectified before supplied to the load (Battery) of 100 Ω resistance.

The high frequency DC-AC inverter formed with IGBT inverted the dc supply into high frequency AC and then this inverted signal is fed to primary coil. The two gate pulses are given to the high frequency inverter section for its operation to produce high frequency AC.

To get the required high DC voltage at the output, DC-DC Boost converter is used which helps to obtain the required output voltage by varying the duty cycle. In Boost converter MOSFET is used as a switch with 25KHz as switching frequency.

The output waveforms from the simulation model are depicted in the figures below.
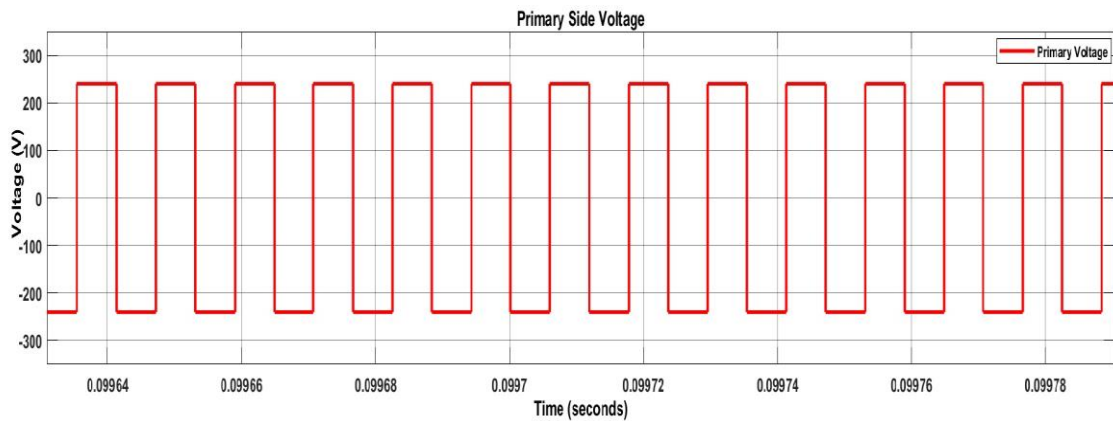
4.4.1 Simulation Waveforms
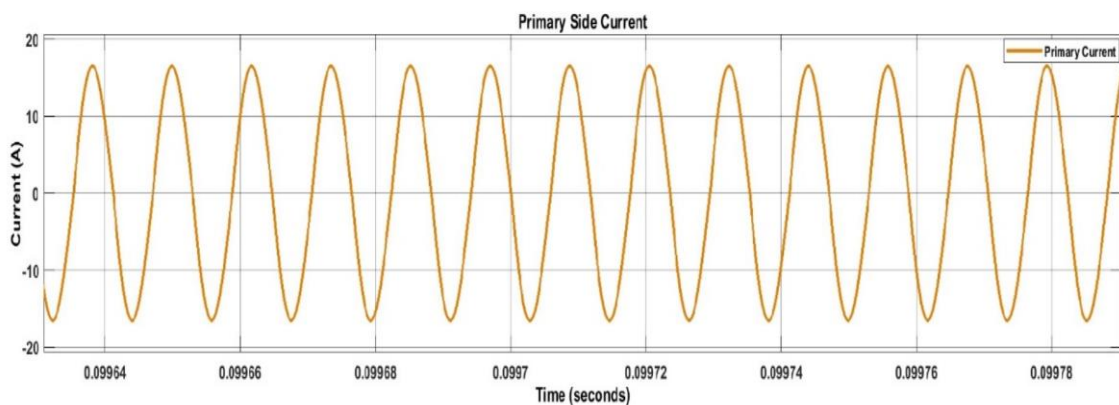

Fig 4.7 Primary side tank capacitor voltage

Fig 4.8 Primary side tank capacitor current

Fig 4.7 and Fig 4.8 shows the primary side tank capacitor voltage of 240 AC with opposite polarity and current value respectively after passing through high frequency DC-AC inverter.
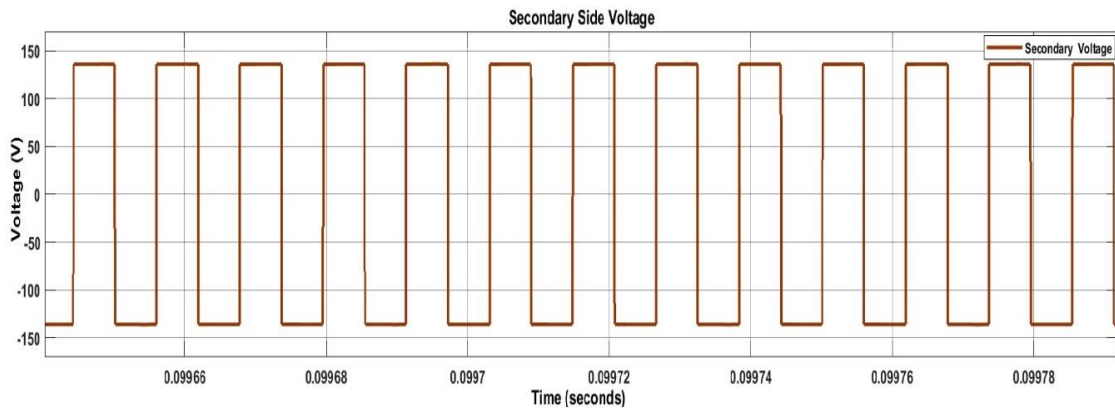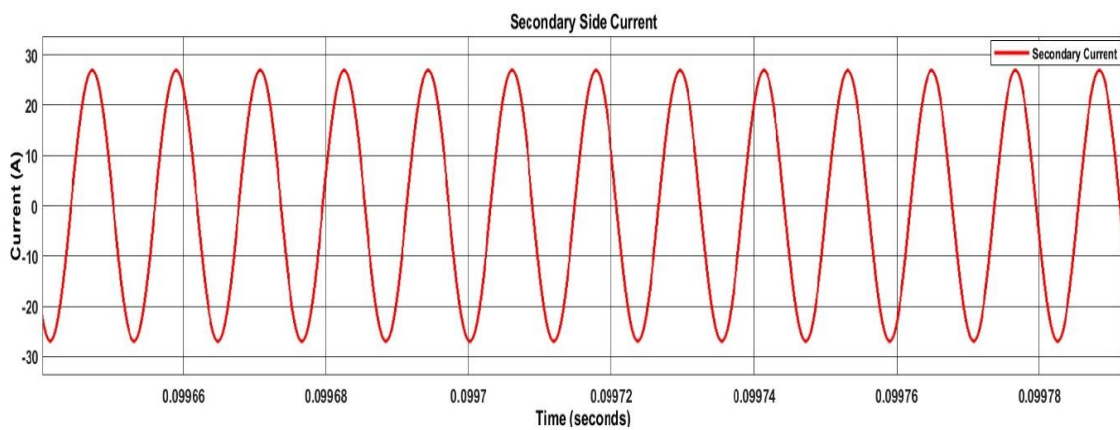
Fig 4.9 Secondary side tank capacitor voltage

Fig 4.10 Secondary side tank capacitor current

Fig 4.9 and Fig 4.10 shows the secondary side tank capacitor voltage of 136 V AC and current of value 27 A respectively.
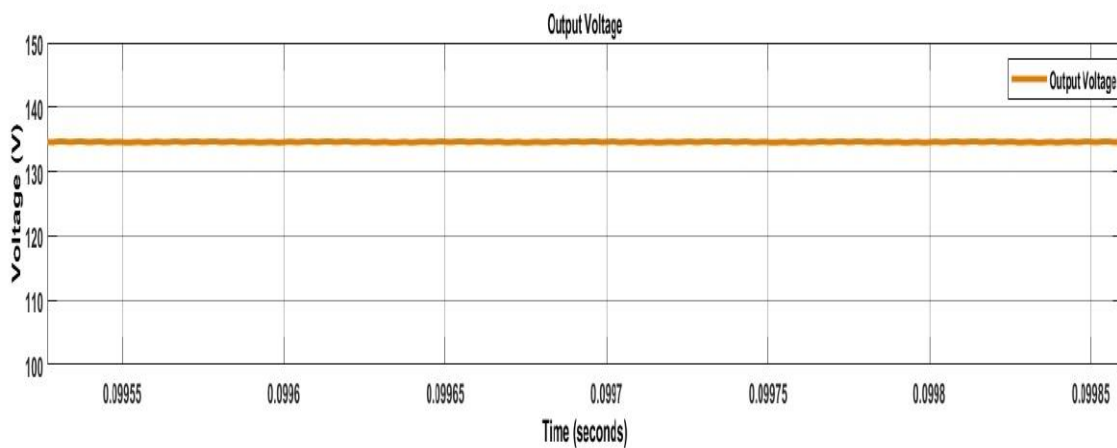

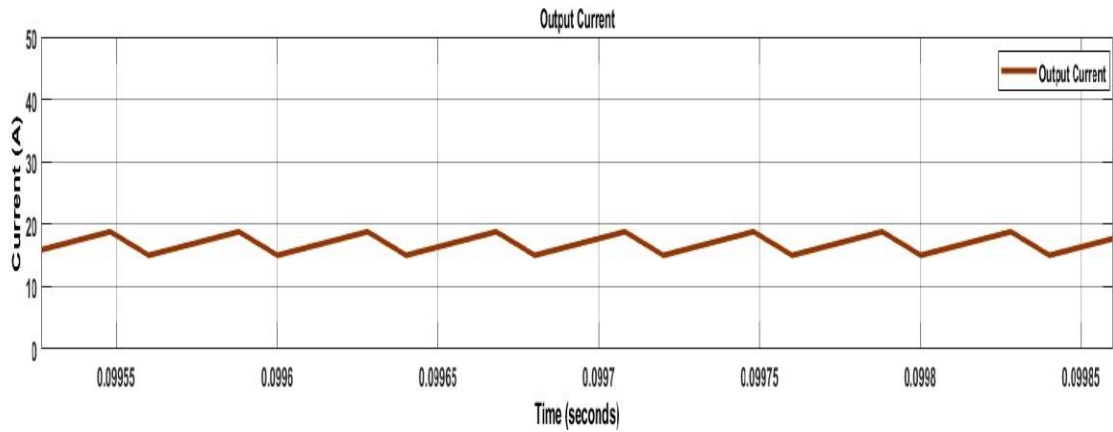Fig 4.11 Output voltage (without boost converter)

Fig 4.12 Output current (without boost converter)

Fig 4.11 and Fig 4.12 shows the output voltage of 135 V DC and current of value 15 A respectively with 100 Ω load. These output voltage and current values are first calculated without adding the boost converter on the load side.

The boost converter used has to be implemented inside the EV, this leads to the additional weight on the EV.
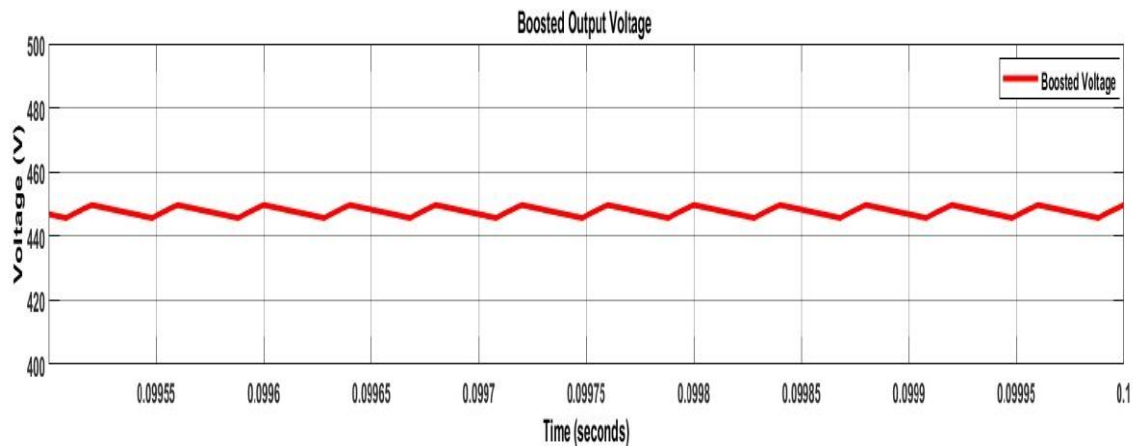

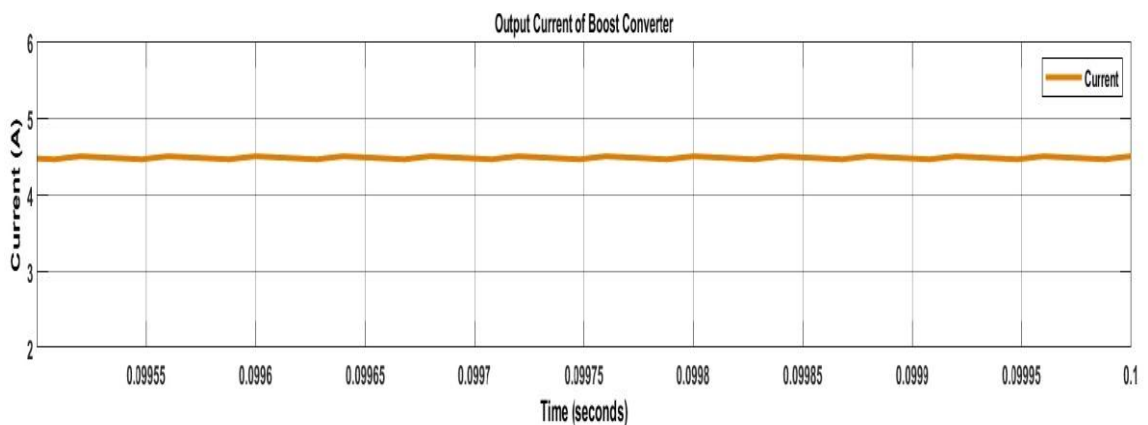
Fig 4.13 Output voltage (with boost converter)

Fig 4.14 Output current (with boost converter)

Fig 4.13 and Fig 4.14 shows the output voltage of 450 V DC and current of value 4.5 A respectively with 100 Ω load. These output voltage and current values are again calculated with adding a boost converter on the load side.

It is observed from Fig 4.13 and Fig 4.14 that both output voltage and current waveforms are smooth, so it becomes possible to get the smoothed output power of the system.
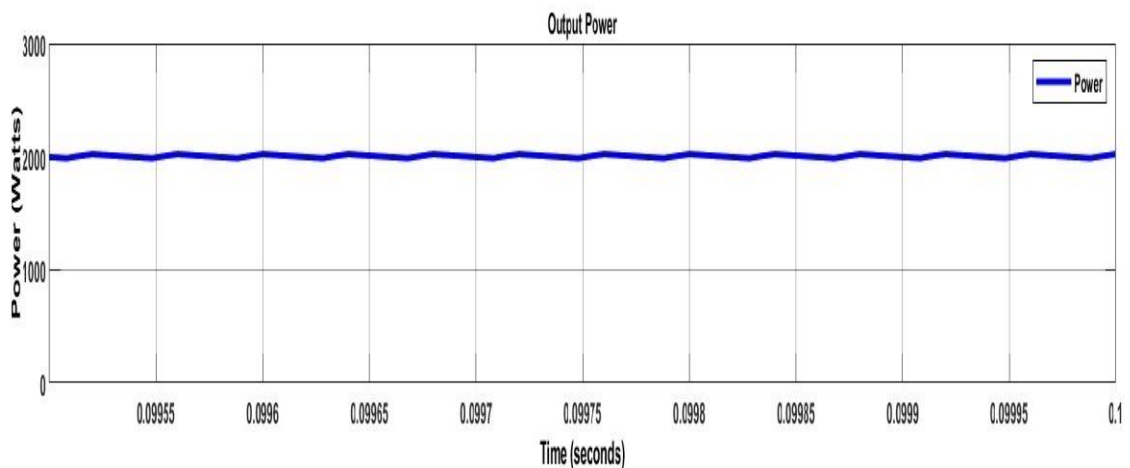
Fig 4.15 Output Power

Fig 4.15 shows the output power of 2 KW with or without adding the boost converter on the load side with 100 Ω load.

Most of the IPT systems needs flow of power in only one direction, which can be achieved by using an AC source at the input side, whereas the AC source is comprising of a high frequency converter at the primary side, and a simple diode bridge at the secondary side. The series compensation type of circuit is shown in above Fig 2.2, having simple design and low cost.

CHAPTER 5

CONCLUSION AND FUTURE WORK

5.1 CONCLUSION

In this work, by the help of Inductive coupling, a WPS system has been designed and the system was implemented/Simulated using the MATLAB/Simulink. The work is a review of wireless charging of EVs. The simulation results are observed with or without adding the boost converter on the load side. The output power observed with or without boost converter is 2 KW with 100 Ω load. It is also observed that by using the boost converter, the output waveforms become smoother, which is very needed for battery charging applications. With the upcoming technology development, this system of wireless charging of batteries of EVs can be brought to reality and also it requires further studies/research.

The design and analysis of a 2KW inductive power transfer system for electric car usage in MVDC networks is carried out. The design is noted to function well at an operating frequency of 85KHz, according to the system's requirements. The higher the operating frequency, the smaller the components size for the hardware implementation of the WPT system. When the system's Quality Factor and the voltage on the transmitting side both declines, the system's performance suffers as the transmitter's capacity to transfer energy to the secondary side suffers as well. The coupling distance cannot be increased to a great extent without lowering performance. As a result, it can be stated that when developed with an operating frequency of 85 kHz, this proposed system provided the intended outcomes, which were validated by simulation results, indicating that this system is suitable for practical applications.

5.2 FUTURE SCOPE

As the WPT System is verified using the MATLAB simulation for 2KW power. Future effort should concentrate on developing and testing the system on a hardware testbed.

REFERENCES

1. Mi, Chris, and M. Abul Masrur. Hybrid electric vehicles: principles and applications with practical perspectives. John Wiley & Sons, 2017.

2. Morris C. The dynamic road ahead: Utah State University builds the nation's most advanced test facility for dynamic wireless charging. Charged EVs: <chargedevs.com>; Nov/Dec 2014. p. 82–7.

3. S. J. Gerssen-Gondelach and A. P. C. Faaij, "Performance of batteries for electric vehicles on short and longer term," J. Power Sour., vol. 212, pp. 111–129, Aug. 2012.

4. V. Etacheri, R. Marom, R. Elazari, G. Salitra, and D. Aurbach, "Chal- lenges in the development of advanced Li-ion batteries: A review," Energy Environ. Sci., vol. 4, no. 9, pp. 3243–3262, 2011.

5. M.A. Rodriguez-Otero and E. O'Neill-Carrillo. "Efficient Home Appliances for a Future DC Residence". In: Energy 2030 Conference, 2008. ENERGY 2008. IEEE. Nov. 2008, pp. 1–6.

6. Stieneker, Marco, and Rik W. De Doncker. "Medium-voltage DC distribution grids in urban areas." *2016 IEEE 7th International Symposium on Power Electronics for Distributed Generation Systems (PEDG)*. IEEE, 2016.

7. Reed, Gregory F., et al. "Ship to grid: Medium-voltage DC concepts in theory and practice." *IEEE Power and Energy Magazine* 10.6 (2012): 70-79.

8. F. Mura and R. W. De Doncker. "Design aspects of a medium-voltage direct current (MVDC) grid for a university campus". In: Power Electronics and ECCE Asia (ICPE ECCE), 2011 IEEE 8th International Conference on. May 2011, pp. 2359–2366.

9. M. Stieneker, J. Butz, S. Rabiee, H. Stagge, and R. W. D. Doncker. "Medium-Voltage DC Research Grid Aachen". In: International ETG Congress 2015; Die Energiewende - Blueprints for the new energy age; Proceedings of. Nov. 2015, pp. 1–7.

10. Porter, Suzanne Foster, et al. "Reviving the War of Currents: Opportunities to Save Energy with DC Distribution in Commercial Buildings." (2014).

11. Bathurst, Graeme, George Hwang, and Lalit Tejwani. "MVDC-the new technology for distribution networks." (2015): 027-5.

12. Rim, Chun T., and Chris Mi. *Wireless power transfer for electric vehicles and mobile devices*. John Wiley & Sons, 2017.

13. N. Shinohara, Y. Kubo, and H. Tonomura, "Wireless Charging for Electric Vehicle with Microwaves," in Proc. of International Electric Drives Production Conference (EDPC), Nuremberg, German, Oct. 2013.

14. Tang, Qinghui, et al. "Communication scheduling to minimize thermal effects of implanted biosensor networks in homogeneous tissue." *IEEE Transactions on Biomedical Engineering* 52.7 (2005): 1285-1294

15. Popovic, Zoya. "Far-field wireless power delivery and power management for low-power sensors." *2013 IEEE Wireless Power Transfer (WPT)*. IEEE, 2013.

16. Kim, Han-Joon, et al. "Review of near-field wireless power and communication for biomedical applications." *IEEE Access* 5 (2017): 21264-21285.

17. J. I. Agbinya et al., ''Size and characteristics of the 'cone of silence' in near-field magnetic induction communications,'' in Proc. MiLCIS, Nov. 2009, pp. 1–4.

18. Lu, Xiao, et al. "Wireless charging technologies: Fundamentals, standards, and network applications." *IEEE Communications Surveys & Tutorials* 18.2 (2015): 1413-1452.

19. Pande, Vishal V., et al. "Wireless power transmission using resonance inductive coupling." *International Journal of Engineering Research and Applications* 4.4 (2014).

20. Dai, Jiejian, and Daniel C. Ludois. "A survey of wireless power transfer and a critical comparison of inductive and capacitive coupling for small gap applications." *IEEE Transactions on Power Electronics* 30.11 (2015): 6017-6029.

21. Waffenschmidt, E., "Wireless power for mobile devices," Telecommunications Energy Conference (INTELEC), 2011 IEEE 33rd International, vol., no., pp.1,9, 9-13 Oct. 2011

22. Rao[1], TS Chandrasekar, and K. Geetha. "Categories, standards and recent trends in wireless power transfer: A survey." *Indian Journal of Science and Technology* 9 (2016): 20.

23. Wheeler, L. P. "II—Tesla's contribution to high frequency." *Electrical Engineering* 62.8 (1943): 355-357.

24. Marincic, A. S. "Nikola tesla and the wireless transmission of energy." *IEEE Transactions on Power Apparatus and Systems*10 (1982): 4064-4068.

25. Shidujaman, Mohammad, Hooman Samani, and Mohammad Arif. "Wireless power transmission trends." *2014 International Conference on Informatics, Electronics & Vision (ICIEV)*. IEEE, 2014.

26. Hou, Chung-Chuan, et al. "Resonant and non-resonant inductive power transfer systems based on planar spiral coils." *2017 IEEE 3rd International Future Energy Electronics Conference and ECCE Asia (IFEEC 2017-ECCE Asia)*. IEEE, 2017.

27. Kim, J., D-H. Kim, and Y-J. Park. "Effective magnetic resonant wireless power transfer system over medium range using an intermediate resonant coil of two loops." *2015 IEEE-APS Topical Conference on Antennas and Propagation in Wireless Communications (APWC)*. IEEE, 2015.

28. Han, Sangwook, and David D. Wentzloff. "Wireless power transfer using resonant inductive coupling for 3D integrated ICs." *2010 IEEE International 3D Systems Integration Conference (3DIC)*. IEEE, 2010.

29. Kurs, Andre, et al. "Wireless power transfer via strongly coupled magnetic resonances." science 317.5834 (2007): 83-86.

30. Jay, Rajiv, and Samuel Palermo. "Resonant coupling analysis for a two-coil wireless power transfer system." *2014 IEEE Dallas Circuits and Systems Conference (DCAS)*. IEEE, 2014.

31. Barman, Surajit Das, et al. "Wireless powering by magnetic resonant coupling: Recent trends in wireless power transfer system and its applications." *Renewable and Sustainable energy reviews* 51 (2015): 1525-1552.

32. Alexander, Charles K., and Matthew no Sadiku. "Electric circuits." *Transformation* 135 (2000): 4-5.

33. Jiang, Chaoqiang, et al. "An overview of resonant circuits for wireless power transfer." *Energies* 10.7 (2017): 894.

34. A. Kurs, A. Karalis, R. Moffatt, J. D. Joannopoulos, P. Fisher, and M. Soljacic, "Wireless Power Transfer via Strongly Coupled Magnetic Resonances," Science, vol. 317, no. 5834, pp. 83-86, June 2007.

35. Lopez, Toni, and Reinhold Elferich. "Method for the analysis of power MOSFET losses in a synchronous buck converter." *2006 12th International Power Electronics and Motion Control Conference*. IEEE, 2006.

36. Shen, Z. John, et al. "Power MOSFET switching loss analysis: A new insight." *Conference Record of the 2006 IEEE Industry Applications Conference Forty-First IAS Annual Meeting*. Vol. 3. IEEE, 2006.

37. C. S. Wang, G. A. Covic, and O. H. Stielau, "Power Transfer Capability and Bifurcation Phenomena of Loosely Coupled Inductive Power Transfer Systems," IEEE Trans. Ind. Electron., vol. 51, no. 1, pp. 148-157, Feb. 2004.

38. S. Schilling, "Ensuring Lead-Acid Battery Performance with Pulse Technology", 1100 South Kimball Avenue, South Lake Texas, 1999.

39. L. R. Chen, "A Design of an Optimal Battery Pulse Charge System by Frequency-Varied Technique," IEEE Transactions on Industrial Electronics, Vol. 54, No.1, February 2007, pp.398.

40. L. R. Chen, "Design of duty-varied voltage pulse charger for improving Li-ion battery-charging response," IEEE Trans. Ind. Electron, Vol. 56, No.2, Feb. 2009, pp.480-487.

41. F. Musavi, W. Eberle, "Overview of wireless power transfer technologies for electric vehicle battery charging," IET Power Electron., 2014, pp.1755-4535.

42. C. Mi. M. A. Masrur, and D.W. Gao, "Hybrid Electric Vehicles: Principles and Applications with Practical Perspectives," Hoboken, NJ, USA: Wiley, 2011.

43. X. Zhang, and C.Mi, "Vehicle Power Management Modeling, Control and Optimization," Berlin, Germany: Springer-Verlag, 2011.

44. Saikot Baroi, Md. Shahidul Islam and Shawon Baroi, "Design and Simulation of a Wireless Charging System for Electric Vehicles," 2nd International Conference on Electrical & Electronics Engineering (ICEEE), 19-21 December 2017, RUET, Rajshahi, Bangladesh.

45. Mohammad Shidujaman, Hooman Samani, Mohammad Arif, "Wireless Power Transmission Trends," 3rd International Conference on Informatics, Electronics & Vision 2014.

46. Siqi Li, and Chunting Chris Mi, "Wireless Power Transfer for Electric Vehicle Applications," IEEE Journal of Emerging and selected topics in Power Electronics, Vol. 3, No. 1, March 2015.

LIST OF PUBLICATIONS

1. Abhishek Shakya, "Implementation of Inductive Wireless Power Transmission System for Battery Charging application", 2022 IEEE Sponsored Second International Conference on Advances in Electrical Computing, Communication and sustainable Technologies (ICAECT 2022), Bhilai, Chhattisgarh, India. (Presented)